NASA Contractor Report 181743

Additional Development of the XTRAN3S Computer Program

C. J. Borland

Boeing Advanced Systems
Seattle, Washington 98124

Contract NAS 1-17864
January 1989

National Aeronautics and
Space Administration

Langley Research Center
Hampton, Virginia 23665-5225

NASA CONTRACTOR REPORT 181743

ADDITIONAL DEVELOPMENT OF THE XTRAN3S COMPUTER PROGRAM

C. J. Borland
Boeing Military Airplane Company
Seattle, Washington 98124

Final Report
Contract NAS 1-17864

January, 1989

NATIONAL AERONAUTICS AND
SPACE ADMINISTRATION
LANGLEY RESEARCH CENTER
HAMPTON, VIRGINIA 23665

TABLE OF CONTENTS

NOMENCLATURE

$\hat{a}$	$= E\xi_x$	(coefficients in Eq. (11))
$\hat{\hat{a}}$	$= \xi_y^2/\xi_x + (2G + H)\xi_y\phi_\eta$	
A	$= M_\infty k^2$	(coefficient in Eq. (1))
b	= total span	
$\hat{b}$	$= F\xi_x^2$	(coefficients in Eq. (11))
$\hat{\hat{b}}$	$= (G + H)\ \xi_y^2$	(coefficients in Eq. (11))
B	$= 2M_\infty^2 k$	(coefficient in Eq. (1))
c	= Local section chord nondimensionalized by Cr	
$\hat{c}$	$= \xi_y/\xi_x$	(coefficient in Eq. (11))
C	= arc length	
C_p	= pressure coefficient	
C_r	= reference chord	
$\hat{d}$	$= G$	(coefficient in Eq. (11))
D_ξ, D_η	= finite difference operators	
$\hat{e}$	$= \xi_y/\xi_x$	(coefficient in Eq. (11))
E	$= 1 - M_\infty^2$	

$\hat{f}$ = $H\xi_y$ (coefficent in Eq. (11))

f_o = $-(A\phi_t + B\phi_x)$

$\hat{f}_o$ = $-(A\phi_t + B\xi_x\phi_\xi)$

f_1 = $E\phi_x + F\phi_x^2 + G\phi_y^2$

$\hat{f}_1$ = $E\xi_x\phi_\xi + F\xi_x^2\phi_\xi^2 + G(\xi_y\phi_\xi + \phi_\eta)^2$

f_2 = $\phi_y + H\phi_x\phi_y$

$\hat{f}_2$ = $\xi_y\phi_\xi + \phi_\eta + H\xi_x\phi_\xi(\xi_y\phi_\xi + \phi_\eta)$

f_3 = ϕ_z

$\hat{f}_3$ = ϕ_ζ

f = instantaneous surface definition

F = $-\frac{1}{2}$ [3- $(2-\gamma)M_\infty^2$] or $-\frac{1}{2}$ $(\gamma+1)$ M_∞^2 (coefficient in Eq. (1))

$\hat{g}$ = $1/\xi_x + H\ \phi_\xi$ (coefficent in Eq (11))

G = $-\frac{1}{2}M_\infty^2$ or $\frac{1}{2}(\gamma-3)M_\infty^2$ (coefficient in Eq (1))

$\hat{h}$ = $1/\xi_x$ (coefficent in Eq (11))

H = $-M_\infty^2$ or - $(\gamma-1)M_\infty^2$ (coefficent in Eq (1))

J = Jacobian in Eq (4)

k = nondimensional time scaling

M_∞ = freestream Mach number

N = number of mesh points

S = area

t = nondimensional time, $kU_\infty T/C_R$

T = physical time

U_∞ = freestream velocity

x = physical streamwise coordinate nondimensionalized by C_R

X = physical streamwise coordinate

X^n = combination of nonlinear terms in Eq (12a)

y = physical streamwise coordinate nondimensionalized by C_R

Y = Physical spanwise coordinate

Y^n = combination of nonlinear terms in Eq (12a)

z = physical normal coordinate nondimensionalized by C_R

Z = physical coordinate

α = angle of attack

β = angle of sideslip

γ = ratio of specific heats

∂ = partial differentiation

δ_ξ, δ_η, δ_ζ = finite difference operators

Δ = difference

ζ = nondimensional transformed normal coordinate

η = nondimensional transformed spanwise coordinate

Λ = sweep angle

ξ = nondimensional transformed streamwise coordinate

τ = nondimensional transformed time coordinate

ϕ = nondimensional pertufation velocity potential function

Φ = physical velocity potential function

SUBSCRIPTS

I	= inboard surface
i,j,k	= indices of potential field matrices in the ξ, η, ζ directions
L	= lower surface
LE	= leading edge
O	= outboard surface
R	= reference
U	= upper surface
x,y,z,t ξ,η,ζ	= partial derivative with respect to given variable
0	= static reference value
∞	= freestream value
$\frac{1}{2}$	= value between mesh points

SUPERSCRIPTS

n	= time level
+	= upper or outboard surface
-	= lower or inboard surface
$\leftarrow$	= backward difference

$\sim$ = first intermediate potential

$\approx$ = second intermediate potential

$'$ = derivative with respect to streamwise direction

$\hat{}$ = transformed value

ADDITIONAL DEVELOPMENT OF THE XTRAN3S COMPUTER PROGRAM

FINAL REPORT -- CONTRACT NAS1-17864
NASA Langley Research Center
Hampton, Virginia

1. INTRODUCTION

The purpose of this report is to describe additional developments and enhancements to the XTRAN3S computer program, a code for calculation of steady and unsteady aerodynamics, and associated aeroelastic solutions, for three-dimensional wings in the transonic flow regime. The program was originally developed by the Boeing Military Airplane Company (BMAC), Seattle, Washington, under Contract F33615-78-C-3201 to the Flight Dynamics Laboratory of the U.S. Air Force Wright Aeronautical Laboratories, entitled "Transonic Unsteady Aerodynamics for Aeroelastic Applications". The final report on that contract was published as AFWAL-TR-80-3107, Vol. I-III. Recently, these reports were updated under a follow-on contract F33615-84-C-3221. The revised final reports have been published as AFWAL-TR-85-3124, Vol. I-III. (Ref. 1-3). These reports provide the basic documentation of the XTRAN3S computer program. Additional work on the program, which is also incorporated in the revised final reports, was performed by BMAC under two NASA contracts, NAS2-10762 to NASA Ames Research Center, "Addition of Boundary Layer Correction Procedures into Transonic Inviscid Codes" (Ref. 4) and NASA-17072 to NASA Langley Research Center, "Further Development of XTRAN3S Computer Program". (Ref. 5)

The present work has been performed under NAS1-17864 to the Unsteady Aerodynamics Branch of NASA Langley Research Center. Funding has been provided by the USAF Wright Aeronautical Laboratories. Work performed under this contract may be summarized by the following list of tasks:

Task 1 – Maintenance and support – The Contractor has provided computer program changes (updates) for error corrections and updates for version control operational on the Langley VPS-32 computer. The XTRAN3S computer program has been installed on the CRAY computer at the Air Force Wright Aeronautical Laboratory and demonstrated by successfully executing a sample case. Consultation with LaRC personnel in applying the program changes has been provided.

Task 2 – Algorithm improvements for the XTRAN3S program have been provided including an implicit finite difference scheme to enhance the allowable time step and vectorization for improved computational efficiency.

Task 3 – A study has been made to determine the feasibility of incorporating configuration effects such as a fuselage, store/pylon, or winglet into the XTRAN3S code. The code has been modified to treat configurations with a fuselage, multiple stores/nacelles/pylons, and winglets.

During the course of the contract, these tasks have been further clarified and defined or modified as a consequence of discussions between the Contractor and the Technical Representative.

The following sections of this report describe the technical and program developments accomplished under the above tasks, and possible future extensions and improvements. Program developments, corrections, etc. have been provided separately in the form of correction sets using the UPDATE program feature of the CDC Cyber series of computers. Appendix A provides modifications to the XTRAN3S User's Manual (Ref. 2).

A FORTRAN listing of the modified code has been provided separately from this report.

2. PROGRAM MAINTENANCE AND SUPPORT

This section of the report will describe error corrections and program maintenance that has been provided during the course of the contract.

2.1 ERROR CORRECTION

During the course of the contract, several minor errors in the XTRAN3S code were discovered and corrected. The following UPDATE Correction sets relating to error correction were developed.

Correction Set		Function
a.	EXTLOFT	Corrects an error in the wing geometry lofting procedure routine GDWING. The error occurred when the loft was extrapolated, i.e., spanwise mesh points on the wing were placed outboard of the last airfoil section definition (Ref. 2).
b.	VISCORR	Corrects an error in the definition of the wedge parameter F in the WEDGEX portion of the boundary layer calculation algorithm. This error was the cause of the surface pressure oscillations seen in the plots of Ref. 4.
c.	FIXPROMAT	Corrects a data input error for input of an inertia matrix in the aeroelastic input routine PROMAT.
d.	MISCFIX	Corrects a logic error in the geometry definition input routine PROCGD, and provides for error trapping and output of a diagnostic warning. Also corrects the pressure and integrated coefficient routines CPRESS and CFOMO to account for the modified grid, and a variable dimension error in ZSWEEP.

e. ENCODE Corrects a labeling error for time history output of aerodynamic coefficients for use on 8-character word machines.

f. VECTCORR Corrects an initialization error in the advanced vectorization UPDATE (described below).

g. PARMGEO Allows for a variable maximum number of points on the airfoil (previously was set at 50).

h. MODEITER Corrects an error to allow for more than one specified modal deflection or motion.

i. FIXDCHK Corrects an error in the DATA CHECK Problem Definition Option.

j. FIXINFI Corrects an error in the Alternate Input File Option so that it operates as documented.

k. FIXEOF Corrects an error which occurred in the event of attempting to read an empty NPRESS or NPREST file.

l. LOFTFIX Corrects an error in the lofting routine GDWING which occurred when the number of airfoil sections defined was identical to the number of spanwise grid points on the planform.

m. SOLVCOR Corrects an error in the vectorized solver routines.

2.2 PROGRAM ENHANCEMENT

Several correction sets were provided which include minor program improvements and additional features, or improve the diagnostic capability of the program. These corrections are described as follows:

Correction Set		Function
a.	BCS17	This correction set has two functions: a) to provide an alternate input file for the input of aeroelastic data, and b) to allow a selective degree-of-freedom matrix to be input for use in aeroelastic solutions with inertia loads when a non-diagonal inertia matrix is input. The use of these two additional features is described in Ref. 1-3.
b.	CONTROL	This correction set provides two additional solution options (tasks) for XTRAN3S: a) Static analysis of a flexible wing with specified modal deflection, and b) Static aeroelastic analysis of a flexible wing with specific modal deflection. [These options can be used to determine static response (i.e., pressures and integrated coefficients) when a specified deflection, such as a control surface is defined.] The aeroelastic option can be used to account for main surface, control surface, backup structure, or actuation system flexibility. Use of these options are described in Ref. 1-3.
c.	INVERR	This provides for output of the generalized mass and stiffness matrices, and the combined aeroelastic matrix and its inverse, for diagnostic purposes.
d.	TASKCORR	This updates the internal documentation for the CONTROL correction set and provides proper branching logic for the additional tasks.

e. INTEQM This provides for the integration of the aeroelastic equations of motion for zero air forces (dynamic pressure set equal to zero), to provide the user a static or dynamic check of the aeroelastic model definition, without the expensive calculation of the aerodynamic pressure coefficients.

f. NEWBL This update removes the effect of calculation of the swept shock position in the calculation of the boundary layer. It has been found (Ref. 6) that this improves the smoothness of the pressure time histories when the viscous boundary layer option is employed. In addition, the correction sets allow for printout of the surface slope modification every 500 steps when the wedge-alone option is employed.

g. SHOCKFIX This provides for proper placement of the shock point when the NEWBL correction is used.

h. VER111 This updates the program banner to the current version, Version 1.11.

i. WRTWRNS This provides additional error diagnostic outputs from several routines.

j. DYNFORC This provides for the input of a sinusoidal dynamic external forcing function similar to the static external force for use in aeroelastic solutions.

2.3 AFWAL CRAY INSTALLATION

During installation of XTRAN3S, Version 1.6, at Wright Patterson Air Force Base, a few subroutines used by XTRAN3S were not found on the system libraries. The correction sets needed to execute XTRAN3S on the system at Wright Patterson Air Force Base are described below.

Correction Set		Function
a.	WPAFB1	Changes subroutine calls to a matrix inversion routine. Deletes calls to subroutines used to audit program usage at Boeing.
b.	WPAFB2	Includes character manipulation subroutines in the library of subroutines used by XTRAN3S.

3. ALGORITHM IMPROVEMENT

During the course of various studies with the XTRAN3S computer program, it has been noted that significant improvement to the computational efficiency and stability of the method could be achieved by various modifications to the algorithm and its implementation. This section of the report will describe and present sample results for two such modifications.

3.1 ADVANCED VECTORIZATION*

The original version of XTRAN3S was developed using the CDC 7600 computer. During the code development period, advanced vector* machines, such as the VPS-32 and CRAY-1S and later the CRAY X-MP became available. The code was adapted to operate on these machines, but only minimal changes to the code were performed to take advantage of "implicit" vectorization, i.e., those portions of the code that could easily be adapted to vector computation through the existing nature of the computational algorithm described in Ref. 1.

Later studies with a pilot code version of XTRAN3S, operational on the CRAY-1S, showed that at least a factor of two improvement in computational efficiency could be achieved by rearrangement of operations to permit a larger degree of implicit (or automatic) vectorization. (This represents a speed-up factor of almost five compared to an unvectorized or scalar code operating on the same machine.) These concepts are generally applicable, but not directly transportable, to the VPS-32 version of the code, since VPS-32 requires longer vectors than the CRAY-1S to achieve improved efficiency when compared with scalar computations. These concepts were discussed in Ref. 5, but not implemented at that time. The improved vectorization scheme has now been implemented on the CRAY X-MP in Version 1.11 of XTRAN3S.

*NOTE: The reader is assumed to be familiar with the concepts of vectorization employed by computers such as the CRAY X-MP and VPS-32.

In this section, the original algorithm of Ref. 1 will be described with respect to its implications for vectorization. Then the modifications necessary to achieve a higher degree of vectorization on the CRAY X-MP will be discussed, and finally the adaptation of those modifications to the VPS-32 will be discussed.

As shown in Ref. 1, the computational algorithm for solution of unsteady transonic flow implemented in XTRAN3S is an alternating-direction implicit (ADI) scheme employing approximate factorization to solve the modified transonic small disturbance potential equation via a finite difference approximation. The original partial differential equation has been replaced by a set of algebraic equations for potential at a finite number of grid points. Starting from a known or given value of the potential ϕ^n at a given time t^n, the solution is advanced to $t^{n+1} = t^n + \Delta t$ via a series of "predictor-corrector" steps. These steps represent three sets of matrix equations, with the solution or "sweep" direction corresponding to a coordinate of the computational mesh. Each equation is solved implicitly for the value of the potential along the sweep direction. The number of equations so solved is the product of the number of points in the computational mesh in the other two coordinates. Thus, if the number of points in the computational mesh in the ξ, η and ζ directions are N_ξ, N_η, and N_ζ respectively, the following represents the number of solutions required to advance the potential solution one step:

ξ - sweep: $N_\eta \times N_\zeta$ equations, length N_ξ

η - sweep: $N_\zeta \times N_\xi$ equations, length N_η

ζ - sweep: $N_\xi \times N_\eta$ equations, length N_ζ

For the η and ζ sweeps, the equations are tri-diagonal, i.e., a matrix formulation has non-zero terms only on the diagonal elements and in elements adjoining the diagonal. The ξ sweep equations are lower quadra-diagonal due to the use of a mixed difference operator, i.e., backward

differences in regions of supersonic flow and central differences in regions of subsonic flow, with a combined shock-point operator.

The solution process for each equation set (sweep) involves four distinct steps: a) formulation of the left-hand side, b) formulation of the right-hand side, c) solution, and d) setting of field and boundary condition values of potential based on this solution.

Since formulation of the left- and right-hand sides are essentially repetitive statements of the finite difference approximations, as are the boundary conditions, these portions are particularly well adapted to vectorization.

The solution process, on the other hand, employs a recursive algorithm and thus cannot be directly vectorized. Several alternate formulations of the solution process, including vectorizable solution algorithms, were evaluated, but proved to provide less improvement in efficiency than the method described below.

In the original version of XTRAN3S, the equations for the ξ-sweep, are solved sequentially for each η mesh point, with a constant ζ mesh point location. Thus for the default values of $N_\xi = 60$, $N_\eta = 20$, and $N_\zeta = 40$, 20 equations of length 60 are solved for each ξ-η plane. Then, for the <u>same</u> ξ-η plane, the η-sweep equations (60 equations of length 20) are solved sequentially in the downstream (increasing ξ) direction due to the presence of the backward spatial or "upwind" difference approximation to ϕ_{xt}. This process is then repeated for the next ξ-η plane in the increasing ζ direction. The ζ-sweep is performed by accessing the data, formulating the equations, and solving for each ξ-ζ plane sequentially in the increasing downstream direction, with the process then repeated for the next plane in the increasing η direction. Since solutions of the ζ-sweep equations, ϕ^{n+1}, are dependent on ϕ^n, ϕ^{n-1} and the solution of the η-sweep equations $\tilde{\tilde{\phi}}$, but not on the solutions to the ξ-sweep equations $\tilde{\phi}$, $\tilde{\phi}$ need not be stored in a three-dimensional array.

The process of the three sweeps for the original scheme and the access of the data from the three-dimensional to two-dimensional arrays, are illustrated in Figure 1.

With the availability of the CRAY X-MP and VPS-32, with features of vectorization and very large available storage, other data arrangement and sweeping schemes have been investigated. In addition, a method for vectorization of the tridiagonal and quadradiagonal solution algorithms has been employed. This method, suggested by the work of J. Lambiotte of NASA Langley Research Center, formulates each step of the tridiagonal or quadradiagonal recursive solution procedure as a vector operation (or vectorizable DO-loop). Since for the η and ζ sweeps the equations are inter-dependent in the ξ direction, reorganization of solutions is required for vectorization.

For the CRAY X-MP, the scheme illustrated by Figure 2 has been adopted. For the ξ-sweep, data is accessed for each ξ-ζ plane (rather than each ξ-η plane), and a vectorized solution is performed in the ζ direction, i.e., each step in the solution is a vector operation of length 40.

This is then repeated for the next ξ-ζ plane, and the intermediate result $\tilde{\phi}$ is stored in a three-dimensional array. For the η sweeps, the data is accessed in the η - ζ planes, and a vectorized solution of length 40 is again performed in the ζ direction, with the results $\tilde{\tilde{\phi}}$ stored in a three-dimensional array. Finally, the ζ-sweeps are performed as a vectorized solution of length 20 in the η direction, and the advanced values of the potential ϕ^{n+1} are stored in place of the values ϕ^{n} at the previous time step. It should be noted that four three-dimensional "levels" of storage, ϕ^{n}, ϕ^{n-1}, $\tilde{\phi}$, and $\tilde{\tilde{\phi}}$ are required for this scheme, compared with three for the original scheme. In addition, however, nine additional three-dimensional arrays for vector equation coefficients and right-hand sides have been stored to improve efficiency and decrease the amount of re-calculation required. For the default mesh, the amount of storage for three-dimensional arrays has increased from 144,000 to 624,000. The total

storage requirement has thus increased from about one-half million words to over one million words. Because of the larger amounts of storage available on both the CRAY X-MP and VPS-32, compared to the CDC 7600, this has caused no difficulty.

Since efficiency on the VPS-32 is improved with long vectors, the following modification to the above scheme could be employed for the ξ-sweep right-hand side setup routine XIRHS. For the ξ-sweep each ξ-ζ plane is treated separately although each of the 800 (=20 x 40) ξ-sweep equations is independent. It is possible to reorganize the ξ-sweep equation setup into a single vector operation of length 48,000. Significant speedup is therefore possible as a comparatively large portion (45 percent) of the computational workload occurs in the ξ-sweep due to the large number of operations performed.

A less complex reorganization would provide for vectorization within each ξ-η plane, thereby providing vector lengths (for the default mesh) of 1,200 (=60 x 20). This modification has previously been implemented by LaRC personnel on the VPS-32 version of the program installed at Langley Research Center.

Additional efficiency can be achieved in the ξ-sweep left-hand side (coefficient matrix) setup routine AMAT, and the η and ζ sweep routines ETARHS, BMAT, ZRHS, and CMAT by replacing the "Double-DO loop" statements in these routine with the explicit vectorization instructions required for the VPS-32. This would provide for vector lengths of 1,200 in the AMAT routine, and of 800 in ETARHS, BMAT, ZRHS, and CMAT, since these routines implement the η and ζ sweep solutions in η-ζ planes sequentially in a downstream marching direction. It is also noted for inviscid solutions, the CMAT routine need be called for only the first complete set of solutions in the ξ-direction as the left-hand side coefficients of the ζ-sweep equations are not modified by subsequent solutions. This modification is not currently implemented.

The above modifications, with the exception of the explicit vectorization language required for the VPS-32, have been implemented in XTRAN3S through use of the UPDATE correction set VECTCRAY presented in Appendix A. This correction set also provides for the additional storage required (and its initialization), modifications required to various labeled COMMON blocks, and an additional subroutine TRISOLZ for the vectorized tri-diagonal solution of the ζ-sweep equations.

A second correction set for vectorization VECT2, also given in Appendix A, modifies the previous correction set to provide for improved computational efficiency. This is accomplished through initial calculation of various combinations of quantities that do not depend on previous solutions, and storage of these quantities for later retrieval and use. Numerous redundant operations in the original code are therefore eliminated, at the cost of additional storage.

3.2 IMPLICIT FINITE DIFFERENCE SCHEME

The governing equation for the XTRAN3S computer program is the modified three-dimensional transonic small disturbance equation for unsteady flow given as follows:

$$\frac{\partial f_0}{\partial t} + \frac{\partial f_1}{\partial x} + \frac{\partial f_2}{\partial y} + \frac{\partial f_3}{\partial z} = 0 \tag{1}$$

where

$$f_0 = -A\phi_t - B\phi_x \tag{2a}$$

$$f_1 = E\phi_x + F\phi_x^2 + G\phi_y^2 \tag{2b}$$

$$f_2 = \phi_y + H\phi_x\phi_y \tag{2c}$$

$$f_3 = \phi_z \tag{2d}$$

where for the various forms of coefficients (described in Ref. 1):

NLR Coefficients:

$$A = M_\infty^2 k^2;\ B = 2M_\infty^2 k;\ E = 1-M_\infty^2;$$

$$F = -\tfrac{1}{2}\ [3-(2-\gamma)M_\infty^2]\ M_\infty^2;\ G = -\tfrac{1}{2}M_\infty^2;\ H = -M_\infty^2$$

or:

NASA-Ames Coefficients:

$$A = M_\infty^2 K^2;\ B = 2M_\infty^2\ k;\ E = 1-M_\infty^2$$

$$F = -\tfrac{1}{2}(\gamma+1)M_\infty^2;\ G = \tfrac{1}{2}(\gamma-3)M_\infty^2;\ H = -(\gamma-1)M_\infty^2$$

ϕ is the small disturbance potential defined from the full potential Φ by

$$\Phi(X,Y,Z,T) = U_\infty C_R\ [x + \phi\ (x,y,z,t)] \qquad (3)$$

where the physical dimensions X, Y, Z, and T have been nondimensionalized by:

$$x = \frac{X}{C_R};\ y = \frac{Y}{C_R};\ z = \frac{Z}{C_R};\ \text{and}\ t = \frac{kU_\infty T}{C_R}$$

where C_R is the wing reference chord and k is a nondimensional scale factor on time.

The following general coordinate transformation may be defined for purposes of re-casting the equations from the physical domain into a more convenient computational domain:

$$\tau = \tau(x,y,z,t);\ \xi = \xi(x,y,z,t);\ \eta = \eta(x,y,z,t);\ \zeta = \zeta(x,y,z,t)$$

Then the governing equation (1) can be written in strong conservation form as:

$$\frac{\partial}{\partial\tau}\left(\frac{1}{J}\hat{f}_0\right) + \frac{\partial}{\partial\xi}\left(\frac{1}{J}\hat{f}_1\right) + \frac{\partial}{\partial\eta}\left(\frac{1}{J}\hat{f}_2\right) + \frac{\partial}{\partial\zeta}\left(\frac{1}{J}\hat{f}_3\right) = 0 \tag{4}$$

where the Jacobian of the transformation is:

$$J = \begin{vmatrix} \tau_t & \tau_x & \tau_y & \tau_z \\ \xi_t & \xi_x & \xi_y & \xi_z \\ \eta_t & \eta_x & \eta_y & \eta_z \\ \zeta_t & \zeta_x & \zeta_y & \zeta_z \end{vmatrix} \tag{5}$$

and

$$\begin{Bmatrix} \hat{f}_0 \\ \hat{f}_1 \\ \hat{f}_2 \\ \hat{f}_3 \end{Bmatrix} = \begin{bmatrix} \tau_t & \tau_x & \tau_y & \tau_z \\ \xi_t & \xi_x & \xi_y & \xi_z \\ \eta_t & \eta_x & \eta_y & \eta_z \\ \zeta_t & \zeta_x & \zeta_y & \zeta_z \end{bmatrix} \begin{Bmatrix} f_0 \\ f_1 \\ f_2 \\ f_3 \end{Bmatrix} \tag{6}$$

In the XTRAN3S program, a stretching-shearing transformation is applied in the streamwise direction to map a general wing planform in the x-y plane into a rectangle in the ξ-η plane. That is:

$$\xi = \xi(x,y);\ \eta = y;\ \zeta = z;\ \tau = t$$

Thus:

$$J = \begin{vmatrix} 1 & 0 & 0 & 0 \\ 0 & \xi_x & \xi_y & 0 \\ 0 & 0 & 1 & 0 \\ 0 & 0 & 0 & 1 \end{vmatrix} = \xi_x \tag{7}$$

and

$$\hat{f}_0 = f_0;\ \hat{f}_1 = \xi_x f_1 + \xi_y f_2;\ \hat{f}_2 = f_2;\ \hat{f}_3 = f_3$$

so

$$\hat{f}_0 = -(A\phi_t + B\xi_x\phi_\xi) \tag{8a}$$

$$\hat{f}_1 = E\xi_x\phi_\xi + F\xi_x^2\phi_\xi^2 + G\,(\xi_y\phi_\xi + \phi_\eta)^2 \tag{8b}$$

$$\hat{f}_2 = \xi_y\phi_\xi + \phi_\eta + H\xi_x\phi_\xi(\xi_y\phi_\xi + \phi_\eta) \tag{8c}$$

$$\hat{f}_3 = \phi_\zeta \tag{8d}$$

since

$$\phi_x = \xi_x\phi_\xi;\ \phi_y = \xi_y\phi_\xi + \phi_\eta;\ \phi_z = \phi_\zeta$$

So the transformed equation can be written in summary form as:

$$\frac{\partial}{\partial\tau}\left(\frac{\hat{f}_0}{\xi_x}\right) + \frac{\partial}{\partial\xi}\left(\frac{\hat{f}_1}{\xi_x}\right) + \frac{\partial}{\partial\eta}\left(\frac{\hat{f}_2}{\xi_x}\right) + \frac{\partial}{\partial\zeta}\left(\frac{\hat{f}_3}{\xi_x}\right) = 0 \tag{9}$$

or in expanded form as

$$\frac{\partial}{\partial t}\left(-\frac{A}{\xi_x}\phi_t - B\phi_\xi\right)$$

$$+\frac{\partial}{\partial \xi}\left\{E\xi_x\phi_\xi + F\xi_x^2\phi_\xi^2 + \underline{G(\xi_y\phi_\xi + \phi_\eta)^2 + \frac{\xi_y}{\xi_x}(\xi_y\phi_\xi + \phi_\eta) + H\xi_y\phi_\xi(\xi_y\phi_\xi + \phi_\eta)}\right\}$$

$$+\frac{\partial}{\partial \eta}\left\{\underline{\frac{1}{\xi_x}(\xi_y\phi_\xi + \phi_\eta) + H\phi_\zeta(\xi_y\phi_\xi + \phi_\eta)}\right\} + \frac{\partial}{\partial \zeta}\left\{\frac{1}{\xi_x}\phi_\zeta\right\} = 0 \qquad (10)$$

The underlined terms in Equation (10) originate with the spanwise (Y-dependent) or cross (X-Y dependent) terms of the original equation, $G\phi_y^2$ and $\phi_y + H\phi_x\phi_y$. The non-underlined terms depend only on original streamwise or normal derivatives. In the XTRAN3S algorithm, the original spanwise term $G\phi_y^2$ was split into streamwise and transformed normal components. These terms were then treated separately with the streamwise component treated implicitly, and the normal component treated explicitly. It has been found in this study that computational stability can be enhanced if the terms are not so split, and the complete term treated in an implicit fashion. This is particularly necessary for cases with strong spanwise flow gradients, such as caused by the presence of external stores. However, for some cases, accuracy may be affected. Therefore use of the unsplit representation of the $G\phi_y^2$ term has been provided as a user option in this version of XTRAN3S.

If equation (10) is expanded and collected in terms of like coefficients, the equation becomes:

$$\frac{\partial}{\partial t}\left(-\frac{A}{\xi_x}\phi_t - B\phi_\xi\right)$$

$$= \frac{\partial}{\partial \xi}\left(\hat{a}\phi_\xi + \hat{b}\phi_\xi^2 + \hat{\hat{a}}\phi_\xi + \hat{\hat{b}}\phi_\xi^2 + \hat{c}\phi_\eta + \hat{d}\phi_\eta^2\right)$$

$$+\frac{\partial}{\partial \eta}\left(\hat{e}\phi_\xi + \hat{f}\phi_\xi^2 + \hat{g}\phi_\eta\right) \qquad (11)$$

$$+\frac{\partial}{\partial y}\left(\hat{h}\phi_\zeta\right)$$

where:

$$\hat{a} = E\xi_x;\ \hat{\hat{a}} = \xi_{y/\xi_x}^2 + (2G + H)\xi_y\phi_\eta;\ \hat{b} = F\xi_x^2$$

$$\hat{\hat{b}} = (G + H)\xi_y^2;\ \hat{c} = \xi_{y/\xi_x};\ \hat{d} = G$$

$$\hat{e} = \xi_{y/\xi_x};\ \hat{f} = H\xi_y;\ \hat{g} = \frac{1}{\xi_x} + H\phi_\xi;\ \hat{h} = \frac{1}{\xi_x}$$

Here $\hat{a}$ and $\hat{b}$ are the original (x-direction) streamwise terms of the governing equation, and $\hat{\hat{a}}$, $\hat{\hat{b}}$, etc., contain coefficients based on the spanwise terms of the equation.

It has been previously noted (Reference 1) that a time-accurate, fully conservative, fully implicit treatment can only be performed on the terms

$$\frac{\partial}{\partial\xi}(\hat{a}\phi_\xi + \hat{b}\phi_\xi^2) \qquad \text{and} \qquad \frac{\partial}{\partial\eta}\left(\frac{1}{\xi_x}\phi_\eta\right)$$

The remaining terms can be differenced in a fully conservative explicit fashion, or in a partially conservative implicit fashion. In the original XTRAN3S algorithm, only the cross-term

$$\frac{\partial}{\partial\xi}(G\phi^2)_\eta$$

is treated in the latter fashion; the remaining terms are treated explicitly.

In the present study, several different combinations of implicit and explicit difference treatments have been investigated. By examining the coefficients in Equation 11, it can be seen that certain terms which were treated explicitly in the original XTRAN3S algorithm can be treated implicitly without loss of accuracy (i.e., without losing the conservation form of the equation). It has also been noted by Batina that only the

original streamwise terms, represented by the coefficients $\hat{a}$ and $\hat{b}$ should be included in the type-dependent difference scheme (defined in Ref. 1) or in the definition of the shock point operator. This treatment of these terms corresponds directly to the original 2-dimensional method of Ballhaus and Goorjian known as LTRAN2.

The modified finite difference alternating direction implicit (ADI) algorithm can this be written for the three sweeps (using the unsplit form of the equations):

i) ξ - sweep:

$$B\delta_\xi\left(\frac{\tilde{\phi}-\phi^n}{\Delta t}\right) = D_\xi\left(\hat{a}^n\,\frac{\tilde{\phi}_\xi+\phi^n_\xi}{2} + \hat{b}\phi^n_\xi\,\tilde{\phi}_\xi\right) + \delta_\xi\left(\hat{a}^n\,\frac{\tilde{\phi}_\xi+\phi^n_\xi}{2} + \hat{b}\phi^n_\xi\,\tilde{\phi}_\xi\right) \qquad (12a)$$

$$+2G\,(\delta_\eta\phi^n)\,D_\eta\,(\overleftrightarrow{\delta}_\xi\phi^n) + \delta_\eta\left(\frac{1}{\xi_x}\,\delta_\eta\phi^n\right) + \delta_\zeta\left(\frac{1}{\xi_x}\,\delta_\zeta\phi^n\right) + \delta_\xi X^n + \delta_\eta Y^n$$

ii) η - sweep:

$$B\overleftrightarrow{\delta}_\xi\left(\frac{\tilde{\tilde{\phi}}-\tilde{\phi}}{\Delta t}\right) = \frac{1}{2}\delta_\eta\left(\frac{1}{\xi}\delta_\eta\tilde{\phi} - \frac{1}{\xi_x}\delta_\eta\phi^n\right) + G(\delta_\eta\phi^n)D_\eta\left(\overleftarrow{\delta}_\xi\tilde{\phi} - \overleftarrow{\delta}_\xi\phi^n\right) \qquad (12b)$$

iii) ζ - sweep:

$$\frac{A}{\xi_x}\left(\frac{\phi^{n+1}-2\phi^n+\phi^{n-1}}{\Delta t^2}\right) + B\overleftrightarrow{\delta}_\xi\left(\frac{\phi^{n+1}-\tilde{\phi}}{\Delta t}\right) = \frac{1}{2\xi_x}\,\delta_{\zeta\zeta}\left(\phi^{n+1}-\phi^n\right) \qquad (12c)$$

where:

$$X^n = \xi_y / \xi_x \phi_\eta^n$$

$$Y^n = \xi_y / \xi_x \phi_\xi^n + H\xi_y \phi_\xi^{n2} + H\phi_\xi^n \phi_\eta^n$$

Here D_ξ is a type-dependent mixed difference operator based on the sign of $(\hat{a}^n + 2\hat{b}\phi_\xi^n)$, δ_ξ is a central difference operator, D_η is a mixed difference operator, D_η is a mixed difference operator based upon the sign of $2G(\delta_\eta \phi^n)$.

This modification of the XTRAN3S algorithm has been implemented in the correction set ALGMOD. Tests of this algorithm modification have shown that a significant improvement in the computational stability of the algorithm has been achieved. The revised algorithm has been tested both on the F-5 wing (as shown in Reference 1) and on the A6-E wing shown in Figure 3. For the A6-E wing, a non-dimensional time step of .01 was required with the original algorithm to achieve a stable converged solution. With the revised algorithm a computational step of .1 could be used. Figure 4 compares the upper and lower surface pressures calculated on the A6-E wing for both the original and revised algorithm. The shock position is displaced slightly upstream (approximately one grid point) for the revised algorithm. Otherwise the results are essentially equivalent. This upstream movement of the shock is considered to be due to the difference in shock-point operator definition in the two versions of the algorithm. That the "fully conservative" nature of the scheme has been preserved is demonstrated by the equivalent shock strength.

For the F-5 wing, a factor of 10 improvement in time step was achieved. With the revised algorithm a fully converged static solution can be achieved in approximately 100 computational steps, corresponding to approximately 25 seconds CP time on the CRAY X-MP (with boundary layer

computation). Equivalent testing has not been performed for unsteady flow cases, but based on past experience, similar improvements should be realized.

3.3 WALL BOUNDARY CONDITION

In the current version of XTRAN3S, the reflection plane "inboard wall" boundary condition, $\phi_y = 0$, was implemented by using a centered finite difference in the transformed spanwise direction, coupled with a backward finite difference in the streamwise direction. In order to implement the centered difference at the reflection plane, a "dummy row" of grid points located inside the wall equidistant to the first row outboard was used. It was noted early in the XTRAN3S development that this formulation tended to be unstable for spanwise grid lines which were swept forward in the physical plane. This instability was present at the spanwise far field boundary for aft-swept grid lines and the current version of XTRAN3S specifies the far-field boundary condition as $\phi_\eta = 0$ which removes the instability. This condition is satisfied identically for grid modifications which provide for unswept grid lines at the spanwise far field boundary (Ref. 7 and 8).

In other studies, it has been noted that use of the condition $\phi_\eta = 0$ at the reflection plane removes the instability due to forward-swept grid lines. It was noted by Batina in Ref. 9 that the proper representation of the grid for the "dummy" points would locate these points by reflection of the wing planform in the physical plane, rather than by extrapolation as was done in the original XTRAN3S code. If the metric coefficient ξ_y were evaluated at the wall using a finite difference formulation, the condition $\phi_y = \xi_y\phi_\xi + \phi_\eta = 0$ would reduce to $\phi_\eta = 0$ identically for a grid with reflected dummy points. In the current version of the code, the metrics are evaluated analytically from the grid transformation (Ref. 5) and thus ξ_y must be set to zero explicitly.

These changes are implemented in the correction set BCWALL. The further modification developed by Batina of curve-fitting the planform edges to be unswept at the reflection plane has not been implemented.

4. GEOMETRIC EXTENSION

This section of the report will describe two modifications for more general geometric capability that have been incorporated in Version 1.11 of the XTRAN3S code. Possible future extensions are described in the following section.

4.1 PYLON-STORE CAPABILITY

In Ref. 9 and 10, two important extensions to the geometric analysis capability of XTRAN3S have been described. Another important feature that has been included in the present study is that of an underwing pylon-store or pylon-nacelle combination, or multiple combinations.

The flutter characteristics of military aircraft with single or multiple external stores has been the most critical aeroelastic problem for this aircraft type. Most aircraft carry speed restrictions for at least some external store configurations. Recent data on the A-6 attack aircraft (Ref. 11) indicate that aerodynamic interference effects may be extremely significant in determining the flutter characteristics. In this section of the report, the implementation of the pylon capability and two versions of an external store capability are described, results presented, and recommendations made. The pylon-store capability has been implemented through the correction sets PYLSTO, PYLON2, STORES2, STORES3 and PARMPS.

4.1.1 Pylon representation

The presence of an external pylon has been simulated in the XTRAN3S code in a manner entirely analogous to that of the original wing representation, i.e. the surface is represented as a discontinuity in the grid, with the surface boundary conditions satisfied at a location midway between grid points. Figure 5 shows a schematic representation of the pylon with respect to an arbitrary set of spanwise grid points. Currently, the pylon representation is restricted to a vertical plane, but is otherwise

unrestricted in location, planform, or thickness, camber, or incidence. If the pylon local surface slopes for the inboard and outboard sides of the pylon are represented by f_I' and f_O' respectively (including the effects of thickness, camber, and incidence), then the pylon boundary conditions are incorporated by substitution of these local slopes for the flow field spanwise derivatives (including coordinate transformation effects). Referring to Figure 5:

Outboard Surface:

$$\phi_{\eta_{JP-\frac{1}{2}}} = f_O' - \xi_y \phi_\xi^+$$

Inboard Surface:

$$\phi_{\eta_{JM+\frac{1}{2}}} = f_I' - \xi_y \phi_\xi^-$$

Where ϕ_ξ^+ and ϕ_ξ^- are the local streamwise derivatives evaluated at the outboard and inboard sides of the pylon.

The first spatial derivatives at the grid points are then evaluated by an average of the neighboring $\frac{1}{2}$-mesh point derivatives weighted by the grid spacing:

$$\phi_{\eta_{JP}} = \left(\frac{\eta_{JP+1} - \eta_{JP}}{\eta_{JP+1} - \eta_{JP-1}}\right) \phi_{\eta_{JP+\frac{1}{2}}} + \left(1 - \frac{\eta_{JP} - \eta_{JP-1}}{\eta_{JP+1} - \eta_{JP-1}}\right) \phi_{\eta_{JP-\frac{1}{2}}}$$

$$\phi_{\eta_{JM}} = \left(\frac{\eta_{JM+1} - \eta_{JM}}{\eta_{JM+1} - \eta_{JM-1}}\right) \phi_{\eta_{JM+\frac{1}{2}}} + \left(1 - \frac{\eta_{JM} - \eta_{JM-1}}{\eta_{JM+1} - \eta_{JM-1}}\right) \phi_{\eta_{JM-\frac{1}{2}}}$$

(If the grid spacing is even, these become simple averages; an equivalent approximation is used in Ref. 10 for fuselage boundary conditions.)

After evaluating the derivatives, these expressions are substituted for local flow field values in both the ξ and η sweeps. The ζ sweep is not affected.

Figure 6 shows the representation of the pylon planform with respect to the grid in a ξ-ζ (vertical) plane. Multiple pylons may be included. The maximum number of pylons is a variable dimension which may be modified by updating and recompiling the source code. The dimension is currently set at two. It may be noted that the pylon representation may also be used to represent a winglet or other vertical surface. If used to represent a canted surface, the effect of cant angle may be accounted for in the input boundary conditions as shown in the schematic of Figure 7.

4.1.2 Store representation - slender body approximation

The effect of external stores on the flow field in the vicinity of a transonic wing could be approximated in a number of ways. The simplest would be to consider the store effect to be concentrated along a single line. This is analogous to the familiar slender body approximation of a line of sources and sinks in linear theory. Because it is deemed most convenient to define surfaces where boundary conditions are satisfied to be located between grid points (in order to avoid double-valued definitions of flow quantities at grid points), the store boundary conditions can be satisfied on a set of four neighboring points, as shown in the schematic of Figure 8. The boundary conditions on the store itself may be defined in a manner entirely analogous to that of the pylon:

Upper and lower surfaces:

$$\phi_\zeta^+ = f_U' - \alpha_s; \quad \phi_\zeta^- = f_L' - \alpha_s$$

Inboard and outboard surfaces:

$$\phi_\eta^- = f_I' - \xi_y \phi_\xi^- - \beta_s; \quad \phi_\eta^+ = f_O' - \xi_y \phi_\xi^+ - \beta_s$$

For the present version, only axisymmetric stores are considered. Therefore:

$$f_L' = -f_U'; \quad f_O' = f_U'; \quad f_I' = -f_U'$$

and α_s, β_s are the angle of attack and sideslip angle of the stores with respect to the free stream.

In the initial evaluation of the pylon-stores modification, described below, it was found that this modification appeared to provide insufficient effect of the store interference on the wing flow field. (Since no store pressure data was available, the aerodynamics of the store itself could not be evaluated.) Because of this insufficient interference, the scheme described in the following section has been adopted.

4.1.3 Store representation - interference shell approximation

In numerous linear theory panel methods, the effects of body interference on lifting surfaces has been approximated by the concept of an interference shell, in which the body surface boundary conditions, predicted by the slender body approximations, are applied at a location in the flow-field more closely simulating the actual body surface than does the body centerline. This was the scheme adopted by Batina in his fuselage interference modification to XTRAN3S described in Reference 10. To simplify the implementation of the scheme, the body surface was approximated by a rectangular shell with surfaces parallel to planes of constant ζ (upper and lower surface) and constant η (side surface). This scheme, as adapted for external stores is shown schematically in Figure 9. A refinement to the scheme is to modify the values of the derivatives applied at the interference shell by approximations based on slender body

theory, in the manner of Reference 10. Along the side boundaries of the interference shell:

$$\phi_\eta^- = \frac{\Delta C}{\Delta \bar{C}} f_I' - \xi_y \phi_\xi^- - \frac{S}{\bar{S}} \beta_s$$

$$\phi_\eta^+ = \frac{\Delta C}{\Delta \bar{C}} f_O' - \xi_y \phi_\xi^- - \frac{S}{\bar{S}} \beta_s$$

and along the upper and lower boundaries

$$\phi_\zeta^+ = \frac{\Delta C}{\Delta \bar{C}} f_U' - \frac{S}{\bar{S}} \alpha_s$$

$$\phi_\zeta^- = \frac{\Delta C}{\Delta \bar{C}} f_L' - \frac{S}{\bar{S}} \alpha_s$$

where the arc length ratios $\Delta C/\Delta \bar{C}$ and the area ratio $S/\bar{S}$ are defined in Figure 9. In a manner similar to the pylon treatment, weighted averages of the local derivatives are used to account for grid spacing. It should be noted that both the pylon and store boundary conditions are applied in an implicit fashion, in a manner identical to that of the main lifting surface.

Multiple stores may be incorporated as well as multiple pylons, and they need not be equal in number. The maximum number of stores is a variable dimension currently set at 2. It should be noted that a faired-over nacelle may be treated in a manner identical to that of a store. The conditions for a flow-thru nacelle have not been implemented in the current version.

4.1.4. Evaluation of pylon-store modification

In order to assess the adequacy of the current approximations to pylon-store modelling, static pressure data on a moderate aspect-ratio attack

aircraft, the Navy A-6E, has been compared with XTRAN3S results for the cases of a clean wing, pylons only, and pylons plus stores for the case of a 400 gal and 300 gal external fuel tank on each wing. The calculations include the effect of a viscous boundary layer and shock-boundary layer interaction at the wind tunnel Reynolds numbers, formulated according to Reference 4. The boundary layer is applied only to the wing, not to the pylons or stores. The wing with stores installed is shown in Figure 10, with the locations of the chords of measured pressures. The experimental data include an AIM-9L Sidewinder missile mounted at an outboard station which has not been included in the XTRAN3S analysis. Due to differences in the inboard boundary conditions (solid wall vs. fuselage plus flow thru nacelle) between the analysis and experiment, and the flexibility of the model wing due to a balance located at the wing fold line, only the pressure data for the region of the wing between the pylons is compared (η = .330). Figures 11 and 12 show the clean wing and pylon only cases for a Mach number of .87 and an angle of attack of 0 degrees. Correlation for these two cases is generally favorable, with the pressure on the lower surface slightly over predicted, especially near the leading edge (typical of small-disturbance method calculations on coarse girds, as shown in Ref. 28). Figure 13 shows the schematic of the grid in the η-ζ plane with the representation of the maximum store diameter for the slender body approximation to the stores on case. Figure 14 shows the pressure comparison for the stores-on case, with the slender body approximation of Section 4.1.1 used in the analysis. It can be seen that the lower surface pressures are not well predicted, with the data showing a negative load over a considerable portion of the wing that is not shown in the analysis.

Figure 15 shows the schematic of the interference shell representation of the stores, and Figure 16 the data comparison. It can be seen that with the interference shell representation, the strength and rearward location of the shock on the lower surface between the pylons is way over predicted. This is an inviscid calculation, whereas the comparison of Figures 11, 12, and 14 included a boundary layer on the wing. The current boundary layer code was not stable for the strong shock predicted.

Examination of the data and analysis suggested that possibly the flow on the store was separated, since the apparent lower surface shock is much weaker and further upstream than the analysis predicts. In order to simulate this effect, a modification to the store geometry was introduced, treating the store as having constant area (and hence zero slope) from just aft of the maximum diameter point to the aft end of the store. This representation improved the comparison by moving the shock upstream and weakening it as shown in Figure 17. The store interference effect is still somewhat overpredicted, although the correlation is improved. Further improvement might be achieved if a more accurate representation of the stores surface were incorporated, as discussd below.

4.2 WING-FUSELAGE CAPABILITY

In order to provide a more complete simulation for comparison of the A-6E pressure data with pylons and stores, it was decided to incorporate the fuselage capability developed by Batina and described in Ref. 10 into the pylon-stores version of XTRAN3S. As an initial effort, the fuselage modification update was added to both the previous Version 1.5 and Version 1.10 of the wing-alone program. It was found that the fuselage update, as received from NASA Langley, considerably inhibited the vectorization of the code for both 1.5 and 1.10 versions. The update was modified so that vectorization was not inhibited. Figure 18 shows a comparison of computation times per iteration, normalized to the value for the unmodified Version 1.5. It can be seen that while the update as received required considerably more computation time for a wing-body case than for a wing alone case, the vectorized update in Version 1.10 permits a wing-body to be run for only a few percent higher cost than a wing-alone run.

Figure 19 shows the schematic representation of the wing-body interference scheme developed in Reference 10. This scheme has been incorporated into the wing-pylon-store version of the XTRAN3S code described above. The resulting code, with wing-fuselage, pylon, and store capability is known as

Version 1.11. Appendix A provides modifications to the User's Manual of Reference 2 necessary for use of Version 1.11.

The AEDC wing-fuselage test problem described in Ref. 10 has been executed successfully. The A-6E wing-fuselage geometry has also been executed successfully, but only after considerable modifications to the geometric slope of the equivalent slender body representing the fuselage. Further, it was not possible to accurately represent the complex A-6E fuselage geometry, which includes a blunt nose, large canopy, and side-mounted engine inlets, with the limited representation available using the modification of Reference 10. A more accurate fuselage representation, as discussed below, is required.

5. POSSIBLE FUTURE EXTENSIONS AND IMPROVEMENTS

This section of the report describes some recommended modifications and extensions to the XTRAN3S code toward the goal of providing a complete aircraft aeroelastic solution capability.

5.1 IMPROVED FUSELAGE-STORE MODELING

The fuselage and store modeling provided in this report was developed by providing a rectangular "interference shell" approximating the fuselage geometry by planes within the rectangular grid. Boundary conditions are satisfied on these rectangular planes by calculating correction factors based on a slender body approximation to the actual body cross section. The interference shell is assumed to extend from the upstream to the downstream limits of the computational grid.

A further refinement to the fuselage interference treatment of Reference 10 is to satisfy the boundary conditions at the nearest grid point adjacent to the body surface. This would provide a more accurate representation since correction by slender body approximations would be minimized. However, two additional complications are introduced: 1) that of additional logic required to determine the indices of the grid points adjacent to the fuselage cross-section at each streamwise station; and 2) satisfying the zero normal flow boundary conditions at points where streamwise grid lines intersect the solid fuselage surface, which may not correspond with the streamwise grid points. Figure 19 and Figure 20 compare these two approaches of accounting for the presence of the fuselage in an XTRAN3S computational grid. Study of a similar approach has been underway at NASA/Ames. Similar modeling could be applied to the store representation.

5.2 MULTIPLE LIFTING SURFACE INTERFERENCE

In addition to the wing-fuselage modification, a multiple lifting-surface (canard-wing or wing-horizontal tail) modification has been developed for

XTRAN3S (Reference 9). Vertical displacement is permitted between the forward and aft lifting surfaces but both must lie in horizontal planes. Results of this modification are promising, but the particular implementation described in Reference 9 is limited as far as practical aircraft configurations are concerned. Actual canard-wing and wing-tail configurations usually have the lifting surface root chords at different spanwise locations due to the presence of the fuselage, and most often have different dihedral angles for the forward and aft surfaces. These effects could be extremely important in accounting for the interference effect due to downwash on the trailing surface. Since the effect of dihedral could be included in new program developments described in Section 5.4 below, this effect could be accounted for in incorporating the multiple lifting-surface capability into XTRAN3S. Another possible complication arises from the fact that in potential methods the wakes are modeled as flat, underformed surfaces. This limitation should be considered in modeling for calculation of downwash interference effects.

5.3 FLOW-THRU/SPECIFIED MASS FLOW NACELLE

In the modification for wing-pylon-store geometry described in Section 4.1, it is assumed that there is no flow through the external store, i.e., the flow equation is not solved for points inside the store and a zero normal flow boundary condition is enforced for grid lines which intersect the surface. For a nacelle, this condition is not correct. Either a flow-thru nacelle condition satisfying continuity (such as for a wind tunnel model) or a specified mass flow condition (simulating the added momentum due to the presence of an engine) should be included. These conditions may be implemented by specifying a flux boundary condition at the entrance and exit planes of the nacelle. It is particularly important that these conditions be handled properly for cases where the nacelle is closely-coupled with the wing, or where the underwing stores are in close proximity to the nacelle. Otherwise the flow that would be entrained must pass to the outside of the nacelle affecting the local flow conditions and possibly the aeroelastic behavior.

This modification is a logical and fairly straight forward extension of the pylon-store capability described in this report. Modification of the wing body capability would provide for a nacelle which is integrated with the fuselage, such as is common for most fighter and attack aircraft. The goal here is, of course, to provide an accurate estimate of the effect of these geometric modifications on aeroelastic behavior, not to assess the performance of the propulsion system itself. Therefore it is felt that the type of modeling described would be adequate and would add to the capabilities of the XTRAN3S code.

5.4 WINGLET/VERTICAL FIN/DIHEDRAL

Probably the most serious deficiency in the existing version of the XTRAN3S code, from the point of view of relating XTRAN3S capabilities to analysis of realistic aircraft configurations, is the lack of ability to incorporate the effects of lifting surfaces which do not lie in planes parallel to the global x-y plane. This would include wings with moderate amounts (more than a few degrees) of dihedral or anhedral, one or more vertical fins (which may be canted with respect to the global x-z plane in the case of multiple fins), winglets (which may also be canted from the vertical direction or not aligned with the freestream direction), or canard or tail surfaces which have differing degrees of dihedral or anhedral from the wing. Almost all practical aircraft configurations incorporate one or more of these features. It is well known, for example, that the effects of cant angle on winglets, or of anhedral on horizontal tails (especially T-tails) are extremely important to flutter characteristics. XTRAN3S cannot currently assess these effects.

The capability for treating winglets, single or multiple vertical fins, and other surfaces with dihedral, could be provided by development of a new "general lifting surface" capability for XTRAN3S. There are several specific features that must be provided in a general lifting surface capability:

a. The ability to incorporate multiple lifting surfaces at arbitrary locations within the computational domain (such as doublet lattice can provide for);

b. The provision of the appropriate coordinate transformations in the x-y, y-z, and x-z planes so that lifting surfaces and their edges will be properly aligned with computational grid lines; and

c. The inclusion of additional nonlinear terms in the governing equations for proper capture of swept shocks in planes not parallel to the global x-y plane.

The first feature is primarily one of "bookkeeping", that is, introducing variable arrays in place of the indices of the current fixed length loops. This has proven quite practical for the case of multiple pylons, for example. An array of the spanwise indices (j) for each pylon station is created, as well as for the initial and final values of the streamwise indices (i) and vertical indices (k) for each pylon. Then at each step of calculating the spanwise flow velocity, additional loops which overwrite this velocity with the appropriate values determined from the pylon surface boundary conditions are executed. Then when the quadradiagonal and tridiagonal equations for the predicted values of the potential are solved, the pylon surface boundary conditions are satisfied automatically. A similar approach can be followed for inserting additional surfaces into the computational grid without much difficulty.

As an illustration of the second feature, Figure 21 shows a cross-section of an aircraft with fuselage, canard with dihedral, wing with anhedral, external store, and winglet. In order to maintain the fundamental nature of the transonic small disturbance solution employed in XTRAN3S, lifting surfaces should be aligned with coordinate planes. In this way the boundary conditions for all lifting surface elements may be treated in a manner similar to the wing in the current XTRAN3S code. Also shown in Figure 21 is the y-z grid system (in the physical plane) necessary to assure this surface alignment. (The grid lines are only shown

schematically so that the plot is not obscured by closely spaced lines.) In Figure 22, the transformation of this lifting surface system to a Cartesian computational space is shown. The transformations for the various segments of the computational space have been developed in a manner entirely analagous to the upstream and downstream stretching that was employed in the x-y plane in the current code. It can also be noted, from Figure 22, that the fuselage and external store surfaces are not aligned with a coordinate plane, but approximated by the nearest adjacent coordinate points, as described in Section 5.1. Although not illustrated, it should also be possible to introduce a modified coordinate transformation in the x-y plane to account for the effects of non-streamwise or pointed tips or winglets not aligned with the freestream, and in the x-z plane to account for winglet and vertical fin sweep.

The introduction of additional nonlinear terms in the governing equations would probably be necessary for the proper capture of swept shocks on surfaces such as winglets and vertical fins. In particular, the terms

$$\frac{\partial}{\partial x}\left(G\phi_y{}^2\right) \text{ and } \frac{\partial}{\partial y}\left(H\phi_x\phi_y\right)$$

in equation 1 were added to the clasical transonic small disturbance equation to properly capture shocks on wings (in the x-y plane) with a sweep greater than about 15 deg. (Reference 12). By analogy, for swept surfaces in the x-z plane, terms for the form

$$\frac{\partial}{\partial x}\left(G\phi_z{}^2\right) \text{ and } \frac{\partial}{\partial z}\left(H\phi_x\phi_z\right)$$

should be included in the governing equations.

The additional out-of-plane nonlinear terms, as well as the transformations, introduce additional coupling terms into the small disturbance equation to be solved. These coupling terms are weighted by the metric of the transformation, which is proportional to the amount of

shearing required in the coordinate system. These additional coupling terms will be treated in a manner entirely analogous to that described in Section 3.2, that is, they are treated implicitly where possible, but add to the explicit portion of the algorithm where an implicit treatment is not possible. Since, however, the shearing required to account for cant angle and dihedral is usually small (typically twenty degrees or less) compared to sweep angles, the overall stability of the computational algorithm is not expected to be affected to a significant degree. If this is not found to be the case, various approximations can be introduced, such as relaxation of the time-accurate conservation formulation for certain terms. Shearing required for winglet and vertical fin sweep can be handled in a manner similar to wing sweep.

An alternative to the generalized form of the small disturbance grid discussed here is the "body-fitted grid system" which is commonly used in full potential, Euler, and Navier-Stokes codes. This grid system, in which a non-Cartesian mesh fitted around the solid surfaces of the aircraft is mapped to a Cartesian computational system, has the advantage of exactly satisfying the surface boundary conditions on the proper physical geometry, thus avoiding the small disturbance approximation. This is outweighed, however, by two huge disadvantages:

a. For a complex configuration, such as an aircraft with multiple lifting surfaces, fuselage, stores or nacelles, etc., the generation of a proper computational mesh is a huge effort in itself, usually requiring numerical solution of sets of partial differential equations, and has not yet become a well-automated process in the general case;

b. For unsteady and aeroelastic problems, the surface motions and deformations require adjustment or recalculation of the computational grid for each point in the solution. This is a cumbersome and expensive process. For continued development of the small disturbance method, therefore, it is felt to be appropriate to provide grid

geometries that are compatible with the assumptions of the flow equations. These may be developed easily for complex configurations by the application of relatively simple algebraic stretching and shearing transformations.

5.5 EMPENNAGE

Development of an empennage capability for XTRAN3S would just be a special case of the multiple lifting surface capability, including the effects of dihedral. Equally important is the effect of the fuselage on the empennage. Recent studies on a transport configuration have shown that the aft closure of the fuselage has a significant effect on the control effectiveness of a moveable horizontal stabilier-elevator configuration, perhaps of the same order as the aeroelastic effect. Therefore, for study of the important characteristics of an empennage, additional configuration features, such as the fuselage closure and the wing-induced downwash should be considered. These would be possible with the modifications to the XTRAN3S code described here.

5.6 CONTROL SURFACE/SYSTEM CHARACTERISTICS

In the current version of XTRAN3S control surface deflections can be accounted for through the use of specified mode shapes, in which the deflection and slope of a control surface segment of a lifting surface such as wing or horizontal tail are simulated by use of a modal deflection. The user must specify the slope (static cases) or slope and deflection (dynamic cases) at each aerodynamic point which occurs on the control surface segment. A minor modification to the code would allow control surfaces to be specified in a more convenient form, i.e., as coordinates of corner points or as percent chord/percent span data. Most of the coding to allow this input is already in place in the input processor. Additional terms need to be incorporated in the static and dynamic boundary condition and aeroelastic solution routines.

An adjunct problem is the specification of control system characteristics, such as the inputs to a sensor, the control law of a feedback system and the frequency response and flexibility (including structural back up flexibility) of an actuator.

These may be specified in the current program by incorporating additional terms and additional degrees of freedom into the generalized mass, stiffness and damping matrices. However, it is up to the user to formulate the control law, sensor equations, and actuator dynamics in terms which may be put directly into the equations of motion. A more general form of specification would be to have the user input control sensor location and type, actuator and feedback system transfer functions, and system flexibility. The XTRAN3S input processor would then modify the dynamic equations of motion and provide for the output of control system and structural dynamic quantities of interest. A similar form of control system data input is permitted by the linear static aeroelastic analysis program FLEXSTAB.

With the capability of specifying control surfaces and control system characteristics explicitly, the XTRAN3S program will be capable of analyzing such situations as automatic flutter suppression systems, stability augmentation systems, or other aeroservoelastic requirements.

5.7 FULL SPAN CAPABILITY

In the current version of XTRAN3S it is assumed that the configuration is laterally symmetric, and a reflection-plane inner wall boundary condition is specified. The code was originally designed to account for either a full-span or half-span (right wing) specification of the geometry. The data necessary to define a full span case is already present in the input geometry processor, and in the index initialization for the spanwise loops. The free-stream "left-hand" wall boundary condition was never specified. A few simple modifications of the current code together with use of the variable dimension feature to provide sufficient spanwise resolution,

should permit a full-span capability to be incorporated in a more advanced version of XTRAN3S. This capability could provide for a more accurate determination of antisymmetric flutter characteristics (taking account of nonlinearties), asymmetric geometries such as an oblique wing, and asymmetric load conditions such as rolling pullout.

5.8 MODAL INTERPOLATION

In the aeroelastic modal data section of XTRAN3S, the natural vibration modes, in the form of deflections and streamwise slopes, must be input at the aerodynamic grid points defined on the surface by the grid definition in the XTRAN3S data set. If this data set is changed, for example to add additional grid points near surface edges for better definition of the pressure distribution, the modal data must be re-interpolated and re-input. A more convenient method of data input is to permit the user input of modal deflections and slopes at the nodes corresponding to the structural geometry in question, and perform the modal interpolation by a method such as surface spline within the XTRAN3S input processor. The source of these modal data will remain the users' choice of structural vibration methods or experimental data. Multiple regions must be allowed to account for discontinuous modal definitions, such as that of elastic control surfaces.

5.9 BALANCED AIRPLANE/JIG SHAPE SOLUTIONS

In the current version of XTRAN3S, the user must specify the undeformed geometry of the aircraft, and a static angle of attack. The airplane is then analyzed as fixed in a coordinate system with reference to inertial space (although specified rigid body motions such as pitch, plunge, and rotation about the fixed system are permitted). An actual static or dynamic aeroelastic loads solution must solve for the airplane equilibrium condition by determining the deformed shape and by balancing the aerodynamic, inertial, and elastic forces. This may be accomplished by introducing additional rigid body degrees of freedom into the equations of motion and simultaneously, a mechanism for balancing those rigid body

degrees of freedom. If a wing alone is considered, it is possible to introduce an artificial "balancing tail load" in which the equations for translational and rotational degrees of freedom are used to solve for the unknown tail lift coefficient at a specified moment arm. For a full airplane problem, however, it is usually necessary to specify a given control surface segment or segments, and couple them to the static or dynamic behavior of the aircraft through some form of control law. The control law could represent a control system, or a simplified representation to force the equations of motion to an equilibrium solution representing, for example, a given structural load factor. Since it is not possible to initially determine the "stability derivatives" in the usual linear sense with solutions of the non-linear equations, an iterative solution is necessary. It should prove possible to include this iterative solution directly in the integration of the aeroelastic equations of motion, once the flow field characteristics are established. If not, solutions at several angles of attack, for example, could be used to establish the initial conditions for the iterative aeroelastic solution.

Another form of iterated solution which should prove highly useful, and can be accomplished in conjunction with the balanced airplane solution described above, is that of determining the "jig shape", i.e., the undeformed, unloaded shape which will correspond to a desired flight loads distribution at a given flight distribution which corresponds to minimizing the induced drag at 1 - g cruise under certain specified structural constraints such as minimum root bending moment. In this solution, the spanwise twist distribution is solved iteratively while the specified lift distribution is maintained. An example of such a solution using XTRAN3S is described in Ref. 13. For fighter aircraft, it may not be sufficient to modify spanwise twist; camber distribution may be modified as well. This could be accomplished by employing a polynomial twist and camber representation and solving for the polynomial coefficients at each section using an iterative solution technique. Polynomial thickness representations could be included in the process (thereby providing an inverse or design mode) but the number of "design variables" required to

reach a specified surface load distribution may require a prohibitive amount of computation.

The use of iterative solutions for balanced airplane parameters and jig shape would provide a useful addition to the current static and dynamic aeroelastic solution capabilities of XTRAN3S.

5.10 DIRECT COORDINATE AEROELASTIC SOLUTION

The original version of XTRAN3S implemented the aeroelastic solution methodology utilizing the "generalized coordinate" or "modal truncation" solution approach, in which it is assumed that the structural deflection under static or dynamic aerodynamic load can be composed of superposition of the natural modes of free vibration. This was done in order to save computation cost (a much smaller matrix solution is performed at each iteration step) and because of insufficient storage. With the use of modern supercomputers such as the CRAY X-MP such restrictions are no longer valid. A comparison of an XTRAN3S modal solution (using 20 truncated modes) for static deflections along the span and at the root of an horizontal tail-elevator system with a direct coordinate solution are given in Figure 23 and 24. It may be seen that while the overall characteristics are duplicated quite well by the two methods, the details of structural deformation are not reproduced well by the modal solution. Both solutions employ a finite element model.

In this example the pressure distribution (also shown in Figure 24) used to load the finite element model for the direct solution was derived from an integration of the pressure from the converged modal solution. The current aeroelastic matrix structure could be modified easily to accept the additional stiffness matrix necessary to implement the direct coordinate solution. Software is available as part of another code to incorporate the integration of pressure distributions to structural node points in XTRAN3S.

5.11 NODAL LOAD/INTEGRATED LOAD SOLUTIONS

The final product for the structural loads analyst is not the pressure distribution but integrated load distributions. These include not only nodal loads which can be directly input into finite element stress analysis, but quantities such as distributions of shear, moment, and torsion with respect to a defined load reference axis. (This is often used in preliminary design even for non-beam-like structure.) Load integration software has been developed for the pilot version of XTRAN3S, and could easily be adapted for installation into an advanced version.

5.12 NEW APPROXIMATE FACTORIZATION ALGORITHM

Recently, it has been reported (Ref. 14) that a new algorithm for solution of the unsteady transonic small disturbance equations, based upon the approximate factorization (AF) algorithm developed by Shanker for the full potential equation (Ref. 15), has been under development by Batina et al at NASA/Langley. Details of the algorithm are described in a NASA document (Ref. 16). Algorithm testing, using a modified version of XTRAN3S, has been reported to show speed improvements of approximately 100 when compared with the current widely disseminated version (Version 1.5) of XTRAN3S. Although no direct comparisons have been made, it can be estimated that the new AF method may offer a speed advantage of about a factor of three over the latest version of the ADI method in XTRAN3S (Version 1.11).

The AF method should be examined further, particularly as it relates to the ease of implementing additional geometric features relative to the current ADI method. Also, a more extensive examination of the potential computational efficiency improvements of the AF method should be performed. If possible, practical, and worthwhile, the AF method should be implemented as an alternative or replacement numerical algorithm in XTRAN3S. Results could then be compared with those obtained using a new code currently under development by NASA/Langley known as CAP-TSD.

5.13 NON-ISENTROPIC EFFECTS/MONOTONE DIFFERENCE SCHEME

Some anomalous behavior of the transonic small disturbance solutions over a narrow Mach number range was first observed in early studies with the two-dimensional code LTRAN2. It was noted that for a Mach number of .88, a two-dimensional symmetric airfoil oscillating about a mean angle of attack of 0^{o} exhibited a non-zero mean lift. If the oscillation were started in the opposite direction, the mean lift had the opposite sign! This was generalized later as a "non-uniqueness" phenomenon (Ref. 17) which is endemic to all transonic potential equation methods. A later study, first with the two-dimensional code XTRAN2L (Ref. 18) and later with XTRAN3S (Ref. 19) showed that the non-unique erroneous solutions could be eliminated by the introduction of entropy correction terms. Also, spurious pressure overshoots at strong shocks could be eliminated by the use of the Enquist-Osher or monotone difference scheme (Ref. 20) in place of the Murman-Cole scheme (Ref. 21). Use of the monotone scheme may also have beneficial effects on code stability. Studies with an earlier version of XTRAN3S showed about a 25% improvement in stability (increase in allowable step size) from using monotone differencing.

5.14 NON-REFLECTING BOUNDARY CONDITIONS

The current version of XTRAN3S uses zero-flux boundary conditions (simulating solid walls) at locations far enough removed from the lifting surface to have negligible effect on the numerical solutions. There has been considerable discussion of the benefits of the use of non-reflective or outgoing-wave boundary conditions in transonic flow solutions. Most of this work has been done in two-dimensions. However, an implementation of non-reflecting boundary conditions has been developed for XTRAN3S (Ref. 22). This modification could be implemented and evaluated for use in future versions of the code. An alternative to use of the non-reflecting boundary conditions is required when the presence of wind tunnel boundaries (solid, porous or slotted walls or free jet) is to be simulated. This modification is discussed in Section 5.15 below.

5.15 WIND TUNNEL WALL CONDITIONS

In the original design of XTRAN3S, several forms of wind tunnel wall boundary conditions were to be permitted. These included solid walls, porous and slotted walls typical of transonic wind tunnels, and free jet (zero pressure differential) wall conditions, in addition to the free stream conditions normally applied. The formulation of these wall conditions is given in Reference 23. These conditions could easily be implemented into XTRAN3S. The porous wall condition has previously been implemented in the pilot code version. This feature would complement the modification for nonreflective boundary conditions discussed earlier.

5.16 SUPERSONIC FLOW

Version 1.11 of XTRAN3S does not operate properly with a supersonic freestream. In some cases, solutions can be produced but they are physically meaningless. In Ref. 24, a modification of the two-dimensional code LTRAN2 was developed by Chow and Goorjian to enable the code to operate with a supersonic freestream, and results are shown up to Mach numbers of 1.35, which is felt to be beyond the practical limit for an isentropic method. The modifications have not been integrated with the non-isentropic correction terms described above, which may extend the practical Mach number range. The modifications, which involve only reformulation of the upstream, downstream, and far field boundary conditions, could be adapted to three-dimensions and implemented in Version 1.11 and evaluated using existing data, such as that shown in Ref. 25).

5.17 IMPROVED BOUNDARY LAYER METHOD

The XTRAN3S code incorporates a two-dimensional quasi-steady boundary layer method based on the Green's lag-entrainment equations, modified by the incorporation of a viscous wedge to simulate the effects on displacement thickness of shock-boundary layer interactions (Reference 4). Although the current method has been shown to provide some improvements when calculations are compared with experimental data, the robustness of the equations, and the computational efficiency with the boundary layer

included, leave much to be desired. Recently, studies by Howlett at NASA/Langley (Reference 26) and by Houwink and Veldman of NLR (Reference 27) have explored alternate methods of coupling the boundary layer and inviscid transonic two-dimensional small disturbance solutions. These methods have shown improved robustness, and in the case of the NLR modification, the ability to handle mildly separated flows. Howlett has extended his method to the three-dimensional code XTRAN3S. This modification could be implemented in Version 1.11 and evaluated. The method of Houwink should also be investigated.

5.18 ALTERNATE GRID TRANSFORMATIONS

In the three-dimensional transonic small disturbance method implemented in XTRAN3S, the equations are transformed to map the coordinates of a swept tapered wing into a rectangular computational planform. Since a single coordinate transformation was employed, the upstream and downstream boundaries in the computational space represented a highly distorted boundary in the physical space. It was determined that this was the cause of a severe limit in the method of obtaining solutions for swept, tapered wings. Therefore, studies were undertaken to reformulate the coordinate transformations so that a rectangular physical space was represented by the computational space, and that the upstream and downstream boundary conditions were properly applied. Three separate transformations were developed and reported in References 5, 7, and 8. The transformation described in Reference 5 is currently implemented in Version 1.11 of XTRAN3S. Other studies have been performed using earlier versions of XTRAN3S with the alternate transformations of Reference 7 and 8. These other grid transformations could be evaluated using Version 1.11 and recommendations developed as to their suitability for advanced versions of the code.

5.19 IMPROVED USER INPUT CAPABILITIES

5.19.1 Arbitrary airfoil coordinate input

Currently, XTRAN3S has two options available to the user to define the airfoil section geometries used in lofting the wing surface:

a. Input of airfoil ordinates and slopes at the aerodynamic grid points; and

b. Input of polynomial coefficients used to define the section geometry.

If the polynomial coefficient option is chosen, the user must derive the coefficients by using a separate pre-processor. If the direct input of ordinates and slopes is chosen, the user must perform interpolation from known points to the aerodynamic grid point locations. Two additional options would enhance the usability of XTRAN3S by removing this additional pre-processing requirements.

a. Input of airfoil ordinates at arbitrary locations along a section with interpolation of the airfoil geometry to aerodynamic grid points performed through a least-squares fitting procedure; and

b. Similar input at arbitrary locations on a section, with interpolation performed through a smoothed cubic-spline fitting procedure.

Both of these procedures have been used successfully in creating airfoil geometry information for XTRAN3S. The smoothed cubic spline procedure, while giving a more accurate fit of the input data, is a more cumbersome procedure. It may require additional evaluation on the part of the user as to the "goodness" of the fit, particularly when the input data is "noisy" such as occurs with the measured surface ordinates of a wind tunnel model (accurate correlation with wind tunnel pressure data often requires this). The least squares procedure has proven very reliable, but may not represent small variations in the data to the degree of accuracy required for correlation studies. The user will also have the option, with either of these methods, of performing the fit separately on the upper and lower surface or of fitting the entire section surface in a single interpolation,

with the trailing edge providing both the initial and terminal points. This procedure has been found in some cases to improve the accuracy of the fit in the leading edge region.

5.19.2 Camber/thickness airfoil input description

Currently airfoil section geometry is described in terms of the upper and lower surface ordinates and slopes. An alternative to this is to input the thickness distribution and camber line definition. The advantage to having this input available is in the use of data that is supplied in this format. Some of the NACA airfoil sections are defined in this way. Sometimes a wing geometry is defined in terms of a standard symmetric airfoil section, with a camber line imposed. The A-6 wing geometry, for example, is defined in terms of scaled standard NACA sections at the root and tip, with a constant camber line superimposed. The alternative to having this input definition available is evaluation of the airfoil geometry on the upper and lower surfaces from the given camber and thickness data as a preprocessing step.

Most of the mechanization of camber/thickness input is already implemented in the XTRAN3S code. A minor modification of the evaluation routine would be required to complete the implementation.

5.19.3 Input data dimensionality

The XTRAN3S data input processor requires that input for both planform geometry and airfoil sections be in nondimensional form. For planform data the program assumes that the planform is nondimensionalized by root chord, and that the wing apex (i.e., intersection of leading edge and root chord) lies at the (x,y) grid point (0.0, 0.0). The airfoil data is assumed to be nondimensionalized by local chord, i.e., in the form z/c vs x/c. A more convenient description, particularly when multiple lifting surfaces or body interference effects are considered, would be a coordinate system of the user's choice. A typical choice of coordinates would be the body station-

wing buttock line-water line system typical of airplane dimensional data. The modification proposed here is to permit separate dimensionality specifications for planform or body geometry, airfoil data, and section attachment data. This is partially implemented in the current XTRAN3S input processor and would require only minor modification to complete.

5.19.4 Alternate geometry input file

Currently, all airplane geometry data is read from the input file. Thus the entire geometry definition is required as input for each run, even a restart of a previous case. A convenient alternative is the use of an alternate file for geometry data. (A similar modification was easily implemented in Version 1.11 for aeroelastic modal data). Data on this file would be in the same format as the input file, but would not appear either in the listing of input files or in the "echo" of XTRAN3S input data. However, the geometry data as read will still be defined in program outputs.

Another use of this option is the creation of XTRAN3S data from an upstream preprocessor, thereby providing a more direct link with project-defined geometry data.

5.19.5 Automatic variable dimensions

In Version 1.11 of XTRAN3S, the maximum problem dimensions (number of grid points in each axis, number of points on the airfoil surface, number of elastic modes, etc.) are set at compile time by a PARAMETER statement. If changing these dimensions is required, e.g. to allow more streamwise or spanwise stations on the wing for improved accuracy or matching of experimental data, a three step process is required:

a. A "Patch" deck is created for UPDATE, which then modifies the appropriate PARAMETER statements in the source code;

b. The source code is re-compiled to form a new object code;

c. The object code is run with new dimensions compatible with those specified by the input data.

When performing grid refinement studies, for example, this is currently a cumbersome procedure. The following method would permit the redefinition of maximum problem dimensions without the necessity of additional user intervention:

a. A preprocessor would be created from several routines of the XTRAN3S input processor;

b. This processor would be used to extract the appropriate "limits" data from the input data deck;

c. If the required limits are different from those currently defined, the program source code will be updated and recompiled. If not, the program will be executed without modification.

These steps could all be mechanized in an automated procedure linked by appropriate Job Control statements. Setting the storage requirements for each execution would also provide more efficient (and therefore less costly) use of available storage.

5.20 IMPROVED PROGRAM OUTPUT CAPABILITIES

5.20.1 Grid transformation data output

The current program does not output the values of x, ξ_x, and ξ_y which are generated by transformation of the grid from physical to computational space. This output is useful in diagnostic procedures when new grid transformation schemes are being evaluated or when numerical difficulties are encountered. They should therefore be added as optional printed

output. (This output is available as part of the Ames grid modification update.)

5.20.2 Alternate pressure output

The current output processor provides for pressure printout in the form of upper surface, lower surface, and pressure difference, at one spanwise grid station per page. An alternate form would print out multiple sections of upper surface pressures on the same page, then similarly lower surface pressures and pressure differences. This "snapshot" format is useful when examining the data for a visual picture of the surface pressure distribution, and provides for less bulkiness in the printed output. It should be made available as an option. For appropriate cases, "snapshot" output of Fourier coefficients could be made available.

5.20.3 Plot file output

Currently, output data from XTRAN3S is made available on two unformatted binary files, NPRESS and NPREST. The NPREST file, especially, is extremely large since it provides surface pressures and all integrated quantities for each iteration or time step. In order to provide data for input to graphics programs, a post processing program has been written to perform this task. The functions of this post processor could be incorporated into the output processor XTRAN3S, so that upon termination of the run, binary coded decimal (BCD) files would be available for direct input into the plotting program of the user's choice. Actual plotting software would not be provided since these are almost always installation dependent.

5.20.4 Flow field analysis output

At the conclusion of an XTRAN3S run, or more often if specified in the data input parameters, the entire state of the XTRAN3S flow field potential, plus the boundary conditions and aeroelastic data, are written to the file NRSTRT. Normally, NRSTRT is rewound each time before it is written, since

the intention was to save only the final flow field state, or an intermediate state in the case of a numerical instability. This file has been used by several investigators to examine the state of the flow field potential calculation, particularly when numerical difficulties have been encountered. Another use of this file would be the calculation of perturbation velocities on surfaces or in the flow field, for purposes such as minimizing the drag of protuberances or the effects of local geometry variations (the PANAIR Code has been used in this way to considerable advantage). Several modifications would be necessary to enable this flow field diagnostic capability:

a. On user option, the NRSTRT file would not be rewound at each SAVE interval;

b. Additional code would be added to the output processor to extract values of the potential and perturbation velocities from the NRSTRT file at the specified intervals, and write them to additional files for printout or for graphical processing. The data to be output could be specified by choosing the plane of the output and the limiting indices within that plane to minimize the volume of information.

5.20.5 Aeroelastic geometry output

Currently, the calculated deflections of a lifting surface are output for either a static or dynamic aeroelastic solution in XTRAN3S. These deflections contain only the aeroelastic portion of the solution, and not the portion due to the wing geometry itself, i.e., that due to thickness, camber, twist, or control deflection. For presentation of aeroelastic results it would be convenient if these outputs both for the undeformed and elastically deformed cases, would be presented in the form of printed and graphical output.

5.21 IMPROVED ERROR HANDLING

5.21.1 Improved input error diagnostics

The XTRAN3S input processor was originally designed with the following features in mind:

a. The input data set would be meaningful, so that data errors could be easily spotted by the user;

b. It would be error tolerant, i.e., typical data input errors such as numbers in the wrong card-image column, data out of order, misspelled words, etc., would not cause fatal program errors (such as occurs with the NAMELIST processor, for example);

c. In the event of detecting an error that could not be accommodated, an error diagnostic would be issued and processing of the input data would be continued with execution inhibited.

The free-field, key-word based input processor developed for XTRAN3S has fulfilled most of these goals. Data sets are meaningful to read without constant reference to the User's manual, once some experience is gained with the program. Data is not dependent on specific card columns, and is generally order-independent (exceptions are noted in the User's manual). However, although allowed for in the code design, not all input error traps were implemented with meaningful error diagnostic outputs. The following steps are recommended:

a. Complete the error diagnostic set for the XTRAN3S input processor, and provide additional traps where necessary;

b. Expand on the messages output to the user including output of the card-image currently being processed, to enable easier correction of the input data;

c. Provide a traceback from the error condition, so that the user could determine which area of the input processor is being executed.

5.21.2 Partial run output

In the event of numerical error occurring during actual program execution the current version of the code terminates without providing for output of the partially completed results. The pressures and integrated quantities are available on the unformatted file NPREST, and if a sufficient number of steps have been processed, on NPRESS at the "Time History Reporting Frequency." These are currently being extracted by a post-processor program. A useful modification to the code would be to provide output of results already completed to the output file, so that in the event of a fatal numerical error partial results can be examined. A similar code modification has already been implemented at NASA/Langley. A possible mechanism for implementing this would be to provide a separate error post processor module, that would perform all output functions regardless of termination conditions.

5.22 IMPROVED VERSION CONTROL

Because of the large number of organizations that have been involved in the development of various features and improvements in XTRAN3S, providing a workable plan for control of the various updates and modifications to the code, and defining the configuration and capabilities of a particular version, have proven difficult. The differences between the Cray computers in use at Boeing, NASA/Ames, and AFWAL and the Cyber VPS-32 at NASA/Langley have also caused difficulty in coordinating code versions and capabilities. Furthermore, the use of different front-end machines at various installations (Cyber 175 vs VAX, for example) has also caused difficulties, especially in providing equivalent versions to various sites that can be updated and maintained. The need for an improved version control plan for XTRAN3S has become evident.

The following version control plan is recommended:

a. The Baseline version of the XTRAN3S code will be Version 1.11. This version, which contains the algorithm and vectorization improvements described earlier, provides a significant enough improvement in efficiency (20 to 30 times Version 1.5) to warrant the use of these improvements in further studies. Version 1.11 is being made available to AFWAL, NASA/Ames, and NASA/Langley.

b. The various previously developed capabilities, as discussed above would be modified as necessary to be compatible with this version (it has already been determined that the Ames grid transformation is compatible with Version 1.11 with only minor modifications).

c. The Version 1.11 code with additional capabilities incorporated, would be re-sequenced and placed under UPDATE control on the Cray system. This would assure that all future updates will be compatible regardless of the front-end machine used. This version would be designated as Version 2.0.

d. Any additional capabilities and any necessary modifications to the existing additional capabilities, would be developed as Cray UPDATE correction packages to be used with Version 2.0. Each UPDATE correction package would follow the "internal documentation" and "structured program design" guidelines under which the original XTRAN3S code was developed. This would assure that traceability of the correction sets is continuously maintained, and that updated program documentation can be maintained. The resulting version of the code would be released as Version 2.1.

e. A "release tape" would be prepared for Version 2.1 and any subsequent program releases. The "release tape" would contain, at a minimum:

    1. Old program library (i.e., UPDATE format) for version 2.0;

2. UPDATE correction set to get version 2.1 from version 2.0;

3. Control cards to extract and update the program and library from the old pl.;

4. Control cards to compile the program under CFT;

5. Control cards to compile the library under CFT;

6. Compile file for version 2.1 program on Cray X-MP computer;

7. Compile file for version 2.1 library on Cray X-MP computer;

8. Control cards and data set to load and execute a sample problem;

9. Control cards which generated the tape;

10. A CATLIST of the tape.

f. A "release memo" should be prepared for Version 2.1 and any subsequent program releases. This "release memo" should contain, at a minimum:

1. An engineering description of the changes or improvements;

2. A listing of the UPDATE correction set;

3. A listing of the output from UPDATE, showing the effects (deletions, insertions) of the correction set; and

4. A FORTRAN listing of the subroutines affected. Where this is not practical, a complete listing of the new version of the code can be obtained from the version release tape described above.

We do not currently address a similar implementation of version control procedures for the VPS-32 system at NASA/Langley due to the differences between the VPS-32 and Cray machines, and the lack of a machine at Boeing similar to the VPS-32. The source code and UPDATE correction sets could be provided on magnetic tape in a compatible format for the VPS-32 system, however.

APPENDIX A
USER'S MANUAL UPDATES

This section of the report will describe additions and modifications to the XTRAN3S User's Manual, AFWAL TR-85-3124, Volume II (Ref. 2), which are necessary to execute the program improvements described in the sections above. These modifications will be described with reference to the various data sections as defined in Section V in Reference 2.

2. COMPUTATIONAL CONTROL SECTION

6) (MODIFIED EQUATION FORM: [NLR, UNSPLIT, AMES])

If MODI: NLR or MODI: UNSPLIT are specified, the forms of the small disturbance equation coefficients described in Section 3.2 are used. If MODI: AMES is specified, the coefficient G is split into normal and streamwise components as follows: $G = G_N + G_S$

where

$$G_N = \tfrac{1}{2} (\gamma - 1) M_\infty^2 - 1; \quad G_S = 1 - M_\infty^2$$

The default is MODIFIED EQUATION FORM: AMES

4. GEOMETRY SECTION

The following data items are added at the end of the geometry data input description:

29) PYLON DEFINITION

The data record indicates that the pylons definitions will follow. (Refer to Figures 5 and 6 for definitions of the index parameters.)

30) NUMBER OF PYLONS: npylns

Input the number of pylons to be defined. A complete set of the following statements (31-38) must be included for every pylon.

31) ETA STATION: jmp

Input the η station index located inboard of the pylon location (which should be equidistant between stations).

32) Z STATIONS: kmnp, kmxp

Input the minimum and maximum Z station of the pylon lower and upper edges (assumed to lie along Z = constant lines in X-Z planes).

33) LEADING EDGE: $imnp_{k1}$, $imnp_{k2}$,...

Input the ξ station indices (i) of the leading edge of the pylon, one for each k index from kmnp thru kmxp.

34) TRAILING EDGE: $imxp_{k1}$, $imxp_{k2}$,...

Input the ξ station indices (i) of the trailing edge of the pylon, one for each k index from kmnp thru kmxp.

35) INBOARD SLOPES

The data record indicates that the surface slopes f'_I of the inboard surface of the pylon follows.

36) The format for the pylon slope data is as follows:

$fypi_{imnp}$, kmnp, $fypi_{imnp+1}$, kmnp,....., $fypi_{imxp}$, kmnp

fypi$_{imnp}$, kmnp+1,....., fypi$_{imxp}$, kmnp+1

⋮

fypi$_{imnp}$, kmxp,....., fypi$_{imxp}$, kmxp

Note that there is one complete data record (not ending with the continuation character +) for each Z station, i.e., from imnp to imxp. If more that one input line is necessary for the data for a given Z station, then the continuation character + should be used. If the leading and/or trailing edges of the pylon are swept (or otherwise vary) with respect to the ξ = constant vertical gridlines, then there may be a different number of input slopes for each record, equal to imxp - imnp+1.

37) OUTBOARD SLOPES

This data record indicates the surface slope f_o' of the outboard surface of the pylon follows.

38) The format for outboard slope data is the same as that for inboard slope data.

39) STORES DEFINITION

This data record indicates that the stores definition will follow.

40) NUMBER OF STORES: nstors

Input the number of stores to be defined. A complete set of the following statements (41-47) must be included for every store.

41) ETA LOCATION: yloc

Input the actual η location (in the nondimensional coordinate system) of the store centerline to be described. This data record must

precede all others used to define a particular store. All other data records used in the definition of a particular store are independent of order (except as noted).

42) SHELL DEFINITION: jmns, jmxs, kmns, kmxs

This data record defines the interference shell indices (shown in Figure 9 as jmn, jmx, kmn, kmx) for the store. If this data record is omitted, the interference shell is calculated by the program to be defined by the mesh points closest to, but outside of, the maximum radius of the store. This is the only optional data record in a store definition.

43) NUMBER OF POINTS UPSTREAM: nupst

Input the number of ξ mesh points upstream of the initial mesh point defining the store.

44) INCIDENCE ANGLE: alphst

Input the incidence angle of the store in degrees (with respect to the wing surface angle of attack).

45) Z LOCATION: zloc

Input the actual Z location (in the nondimensional coordinate system) of the store centerline.

46) RADII: $ryzs_{1,n}$, $ryzs_{2,n}$,.....+
.....$ryzs_{npst,n}$

Input the radii of the nth store at each of the streamwise (ξ) grid locations along the store centerline. These locations must be calculated from the store geometry using the grid transformation

$\xi(x,y)$ in current use (e.g., Refs. 5, 7, or 8). The current version of XTRAN3S (Version 1.11) uses the transformation of Ref. 5. The number of points in this record (npst) defines the number of points on the store.

47) SLOPES: $fyzs_{1,n}$, $fyzs_{2,n}$,.....+
..... , $fyzs_{npst,n}$

Input the radius slopes dr/dx of the nth store at the same streamwise (ξ) grid locations.

48) FUSELAGE DESCRIPTION

This data record indicates that the fuselage description follows.

49) MAXIMUM RADIUS: rmax

Input the maximum radius of the fuselage (nondimensional coordinate system).

50) ANGLE OF ATTACK: alphaf

Input the fuselage angle of attack (in degrees) with respect to the wing reference plane (negative of the wing incidence angle).

51) TOP BC GRIDLINE: kbcu

Input the upper gridline of the fuselage interference shell (k_t in Figure 19).

52) BOTTOM BC GRIDLINE: kbcl

Input the lower gridline of the fuselage interference shell (k_b in Figure 19).

53) SIDE BC GRIDLINE: jbcr

Input the outboard gridline of the fuselage interference shell (j_s in Figure 19).

54) NUMBER OF GRIDPOINTS UPSTREAM: nfusup

Input the number of ξ mesh points upstream of the initial mesh point defining the fuselage.

55) TOP: nintpts, +

xf_1, ... xf nintpts +
rf_1, ... rf nintpts +
drf_1, ... drf nintpts

where: nintpts = number of ξ grid points defining the fuselage;

xf_n = ξ locations of the fuselage grid points (must correspond to defined ξ - mesh);

rf_n = fuselage radius (nondimensional coordinates) at the corresponding ξ location;

drf_n = fuselage slope at the corresponding ξ locations.

Note that the data records (48-55) are order dependent and all must be included if a fuselage is defined.

6. STRUCTURAL MODAL SECTION

In this and the following section, capability of defining a dynamic (time varying) external forcing function has been included for dynamic aeroelastic analysis tasks. The following data records are modified:

4) (NUMBER OF [STATIC, DYNAMIC] EXTERNAL FORCES: nefaes or nefaed)

The number of static or dynamic external forces to be considered in the aeroelastic analysis. If both are required, e.g., engine thrust and flutter excitation system, both STATIC and DYNAMIC specifications can be specified.

20) EXTERNAL [STATIC, DYNAMIC] FORCE MODAL SECTION

This section indicates that the modal displacement shape for static or dynamic external forces are to be input next. Each mode in the analysis requires one of the following set of records (21-23).

21)-23) Same format as shown in Reference 2.

7. STRUCTURAL MATRIX SECTION

10) [STATIC, DYNAMIC] EXTERNAL FORCE VECTOR

This record indicates that a static or dynamic external force vector will be input. Records 10 and 11 are input only if nefaes $\neq 0$ or nefaed $\neq 0$.

11) The format for a dynamic external force vector is the same as that for a static external force vector, and is given in Reference 2.

11A) EXTERNAL FORCE PHASE: phasef

11B) EXTERNAL FORCE FREQUENCY: freqef

11C) EXTERNAL FORCE AMPLITUDE: amplef

These items defined the phase (in degrees), frequency (in radians/sec), and amplitude (nondimensional factor) of the applied dynamic external force vector. Only sinusoidal time variation is available, and all components of the dynamic external force will be in-phase and at the same frequency.

Items 11A, 11B, and 11C are order - independent.

REFERENCES

1. Borland, C.J., "XTRAN3S - Transonic Steady and Unsteady Aerodynamics for Aeroelastic Applications, Volume I - Technical Development Summary" AFWAL-TR-85-3124 (Vol. I), January, 1986.

2. Borland, C.J., and Thorne, R.G. "XTRAN3S - Transonic Steady and Unsteady Aerodynamics for Aeroelastic Applications, Volume II - User's Manual, "AFWAL-TR-85-3124 (Vol. II), January 1986.

3. Thorne, R.G. "XTRAN3S - Transonic Steady and Unsteady Aerodynamics for Aeroelastic Applications, Volume III - Programmer's Manual", AFWAL-TR-85-3124 (Vol. III), January 1986.

4. Rizzetta, D.P., and Borland, C.J., "Numerical Solution of Three-Dimensional Unsteady Transonic Flow Over Wings Including Inviscid/Viscous Interactions", NASA CR 166561, February 1984.

5. Borland, C.J., "Further Development of XTRAN3S Computer Program" NACA CR 172335, May 1984.

6. Marstiller, J.W., Guruswamy, P., Yang, T.Y., and Goorjian, P.M., "Effects of Viscosity and Modes on Transonic Flutter Boundaries of Wings,: AIAA Paper 84-0870-CP, May, 1984.

7. Guruswamy, P.G., and Goorjian, P.M., "An Efficient Algorithm of Unsteady Transonic Aerodynamics of Low Aspect Ratio Wings", Journal of Aircraft, Vol 22, No. 3, March 1985, pp 193-199.

8. Bennett, R.M., Seidel, D.A., and Sandford, M.C., "Transonic Calculations for a Flexible Supercritical Wing and Comparison with Experiment", AIAA Paper 85-0665-CP, April 1985.

9. Batina, J.T., "Unsteady Transonic Flow Calculations for Interfering Lifting Surface Configuration", AIAA Paper 85-1711, July, 1985.

10. Batina, J.T., "Unsteady Transonic Flow Calculations for Wing-Fuselage Configurations," AIAA Paper 86-0862, May, 1986.

11. Cole, S.R., Rivera, V.A., and Nagaraja, K.S., "Flutter Study of an Advanced Composite Wing with External Stores", AIAA Paper 87-0880, April, 1987.

12. Lomax, H., Bailey, F.R., and Ballhans, W.F., "On the Numerical Simulation of Three-Dimensional Transonic Floor with Application to the C-141 Wing", NASA TN D-6993, August 1973.

13. Borland, C.J., and Gimmestad, D.W., "Aeroelastic Tailoring of High Aspect-Ratio Composite Wings in the Transonic Regime", AGARD Conference Proceedings No. 354, April, 1983.

14. Edwards, J.W., "A Program for Complete Aircraft Aeroelastic Analysis-CAP-TSD", presented to Aerospace Flutter and Dynamics Council, October, 1986.

15. Shankar, V., and Ide, H., "Treatment of Steady and Unsteady Flows Using a Fast, Time-Accurate Full Potential Scheme", AIAA Paper 85-4060, October, 1985.

16. Batina, J.T., "Assessment of an Approximate Factorization Algorithm for Solution of the Three-Dimensional Unsteady Transonic Small-Disturbance Equation", NASA TM 89014, September, 1986

17. Steinhoff, J., and Jameson, A., "Multiple Solutions of the Transonic Potential Flow Equations, "AIAA Journal Vol. 20, No. 11, November, 1982.

18. Fugelsang, D., and Williams, M., "Non-Isentropic Unsteady Transonic Small Disturbance Theory, "AIAA Paper 85-0600.

19. Gibbons, M.D., Whitlow, W., and Williams, M.H., "Nonisentropic Unsteady Three-Dimensional Small Disturbance Potential Theory, "AIAA Paper 86-0863, May, 1986.

20. Goorjian, P.m., and Van Buskirk, R., "Implicit Calculations of Transonic Flows Using Monotone Methods, "AIAA Paper 81-0331, January, 1981.

21. Murman, E.M., and Cole, J.B., "Calculation of Plane Steady Transonic Flows, "AIAA Journal Vol. 9, No. 1, 1971, pp. 114121.

22. Whitlow, W., "Characteristic Boundary Conditions for Three-dimensional Transonic Unsteady Aerodynamics, "NASA TM 86292, October, 1984.

23. Yoshihara, H., "Formulation of the Three-dimensional Transonic Unsteady Aerodynamic Problem", AFFDL TR-79-3030, February, 1979.

24. Chow, L.J., and Goorjian, P.M., "Implicit Unsteady Transonic Airfoil Calculations at Supersonic Freestreams", AIAA Paper 82-0934, June, 1982.

25. Tijdeman, J. etal, "Transonic Wind Tunnel Tests on an Oscillating Wing With External Stores", AFFDL TR-78-194, March 1979.

26. Howlett, J.T., "Efficient Self-Consistent Viscous-Inviscid Solutions for Unsteady Transonic Flow", AIAA Paper 85-0482, January, 1985.

27. Houwink, R., and Veldman, A.E. P., "Steady and Unsteady Separated Flow Computations for Trnasonic Airfoils, "AIAA Paper 84-1610, June, 1984.

28. Anderson, W.K., and Batina, J.T., "Accurate Solutions, Parameter Studies, and Comparisions for the Euler and Potential Flow Equations", AGARD 62nd Fluid Dynamics Panel meeting Symposium on Validation of Computational Fluid Dynamics, Lisfon, May 2-5, 1988.

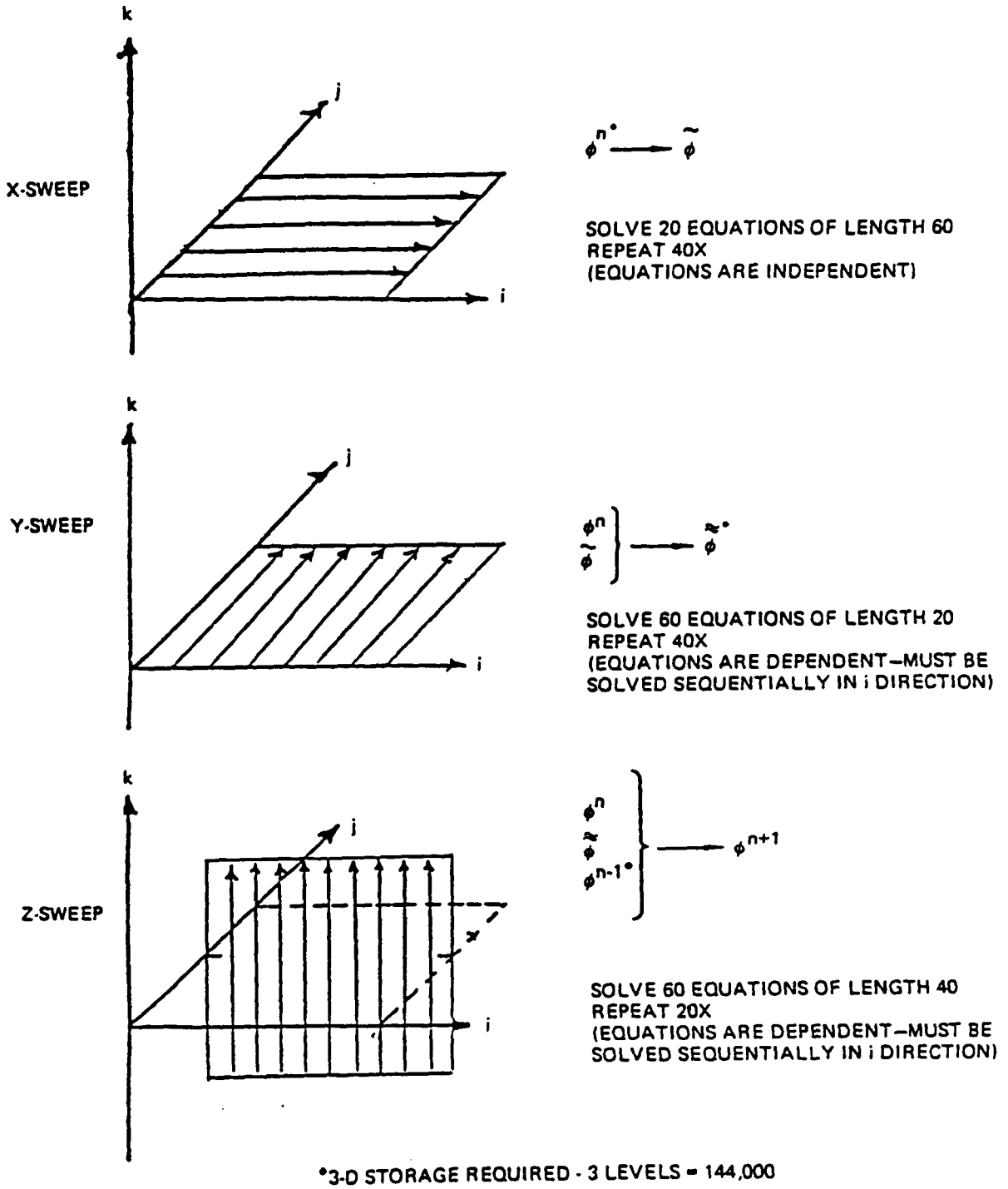

Figure 1. Original Algorithm Storage Scheme

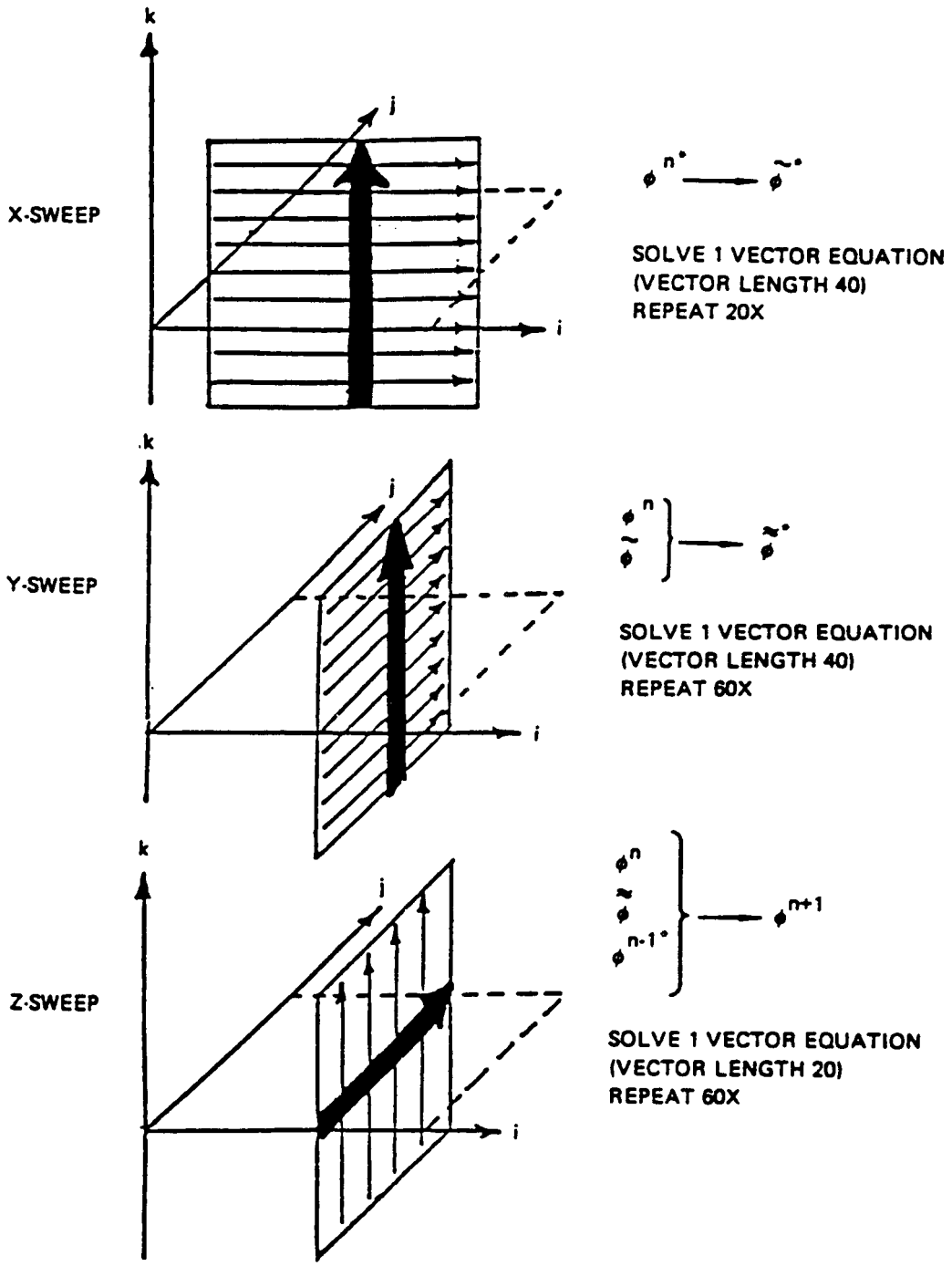

*3-D STORAGE REQUIRED - 4 LEVELS + 9 COEFFICIENTS = 624,000

Figure 2. Modified Algorithm Storage Scheme

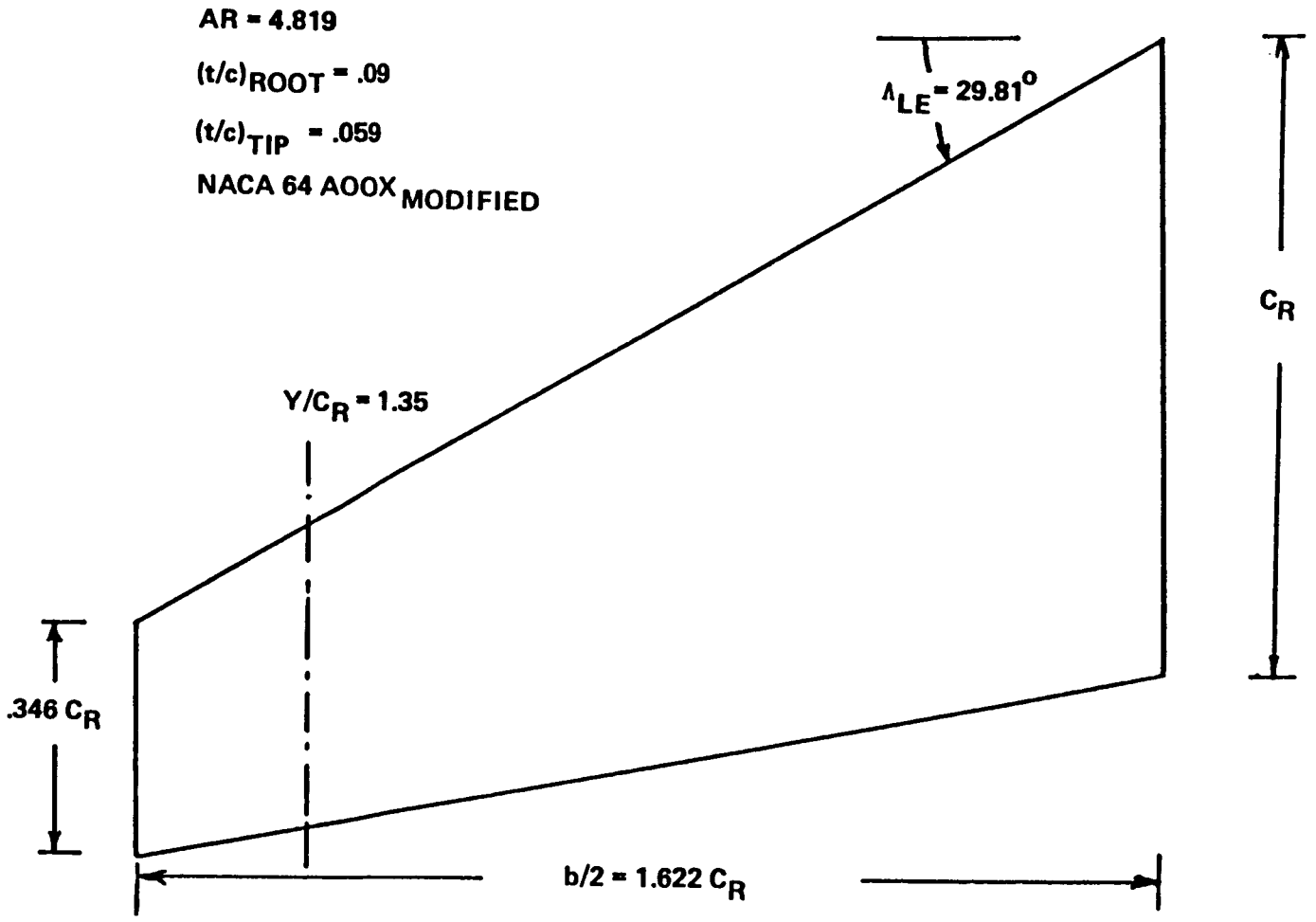

Figure 3. A-6E Planform in XTRAN3S Calculations

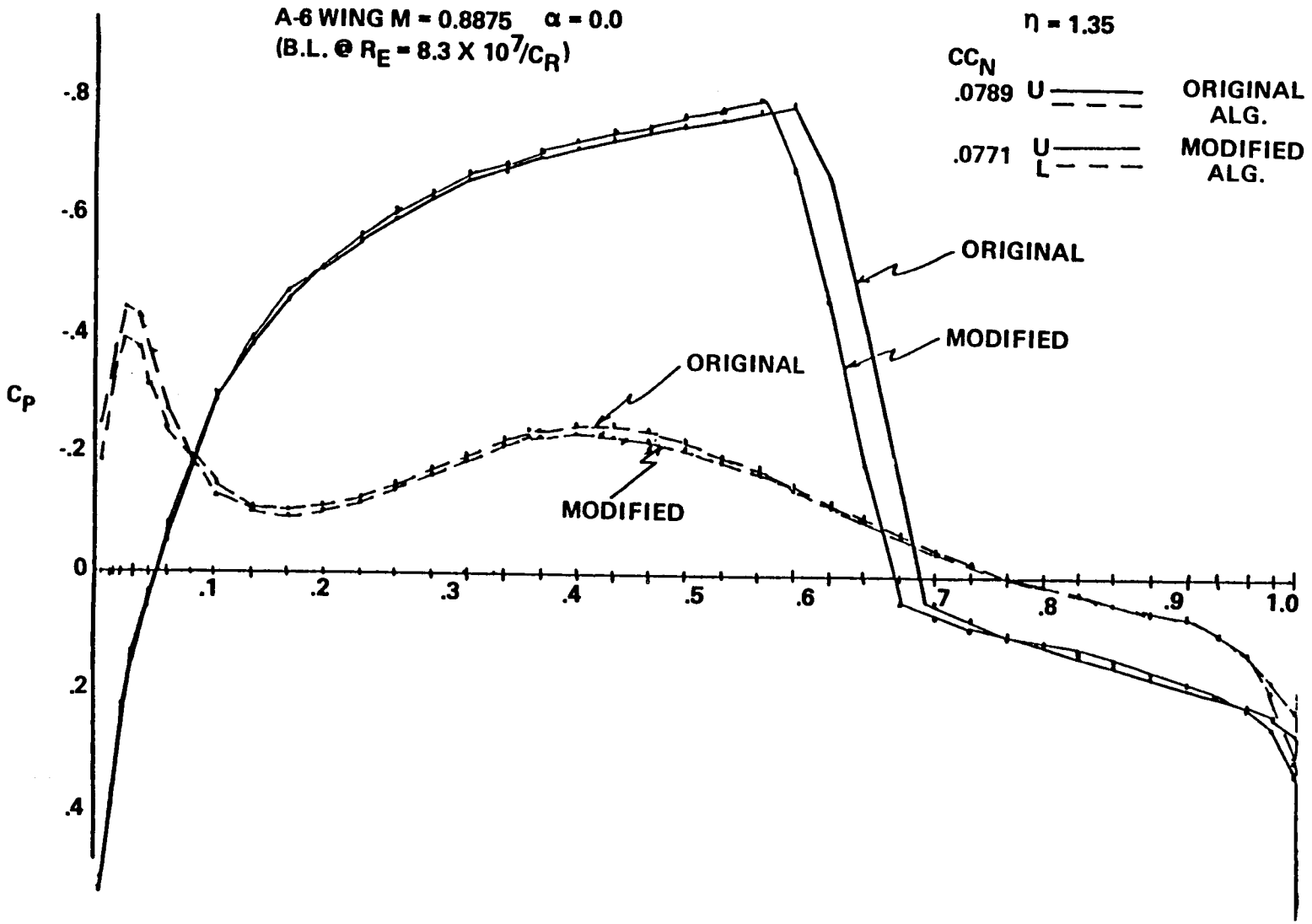

Figure 4. Comparison of Pressure Distribution Calculated by the Original and Revised XTRAN3S Algorithms

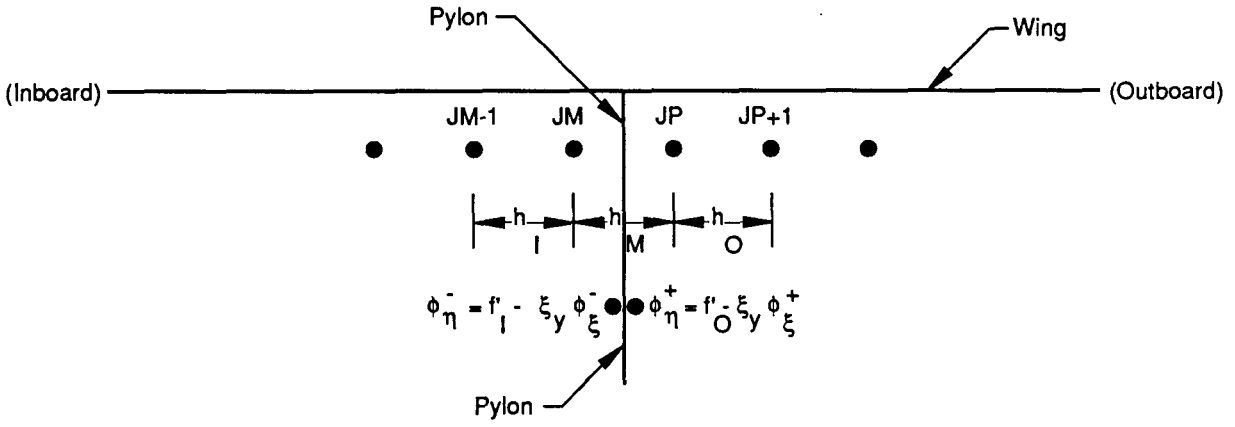

Figure 5. Schematic Representation of Pylon

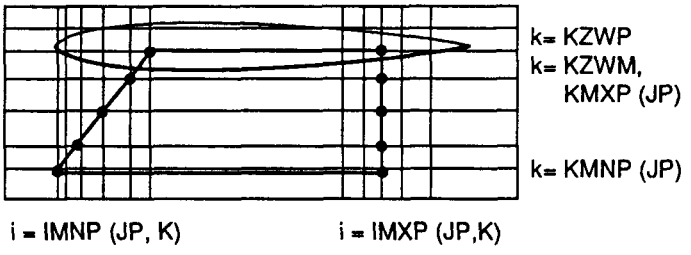

Figure 6. Planform Representation of the JPth Pylon

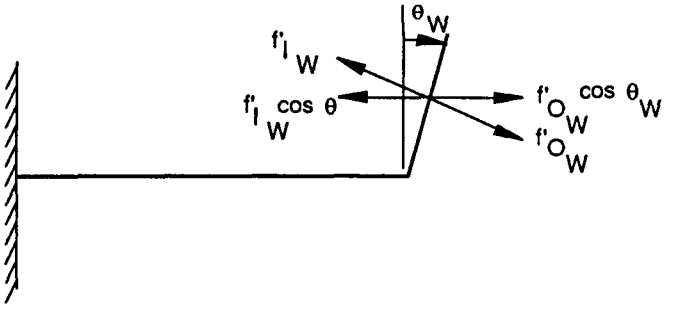

Figure 7. Approximate Representation of Canted Winglet

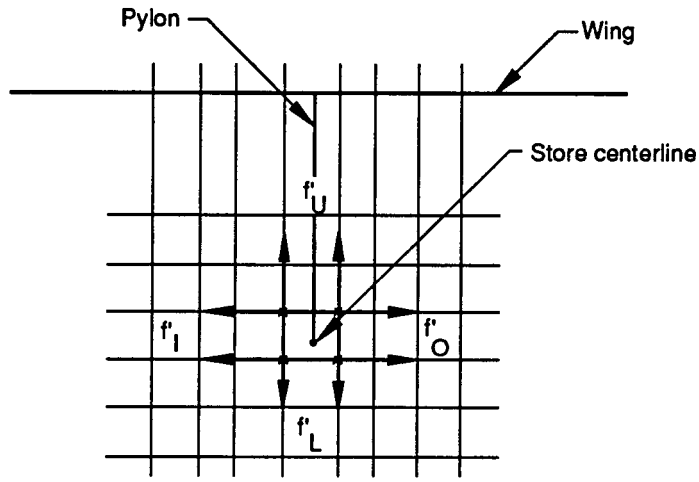

Figure 8. Slender Body Approximation to External Stores

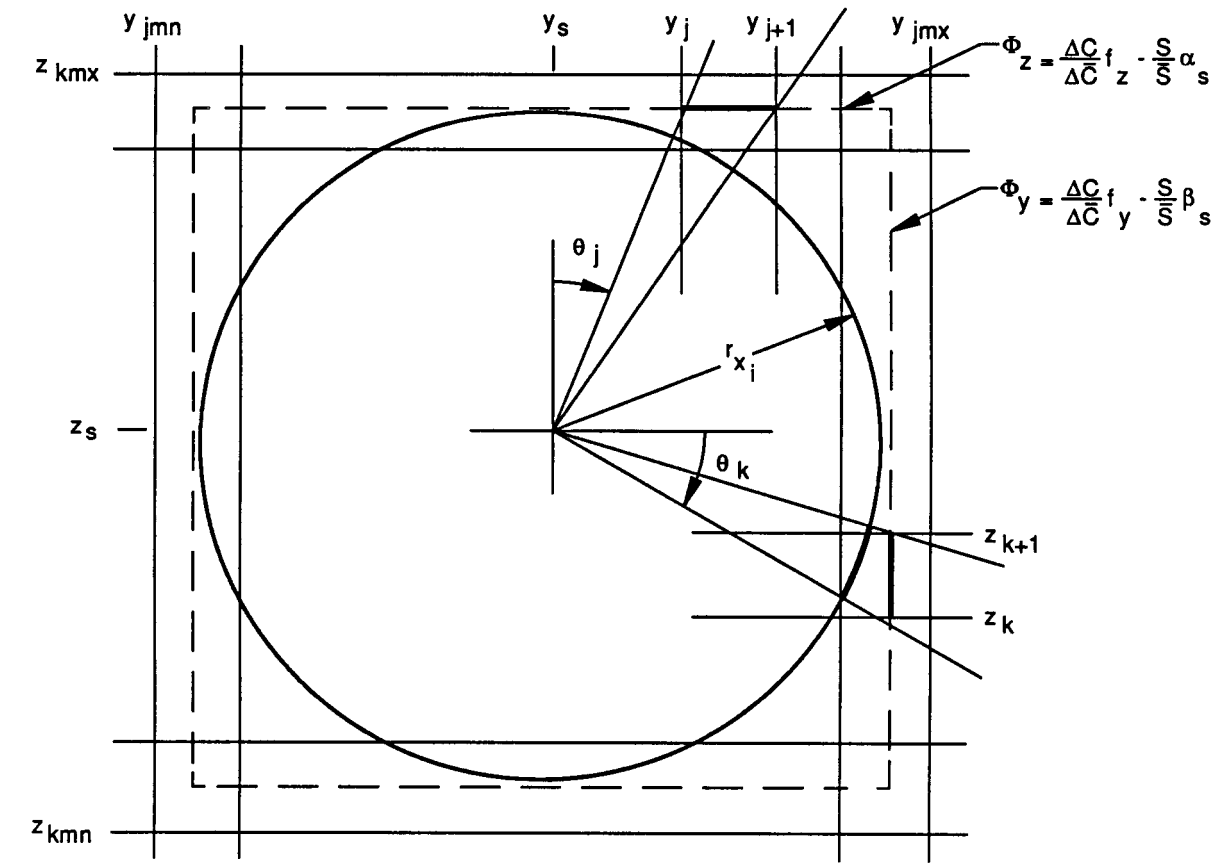

Figure 9. Interference Shell Geometry

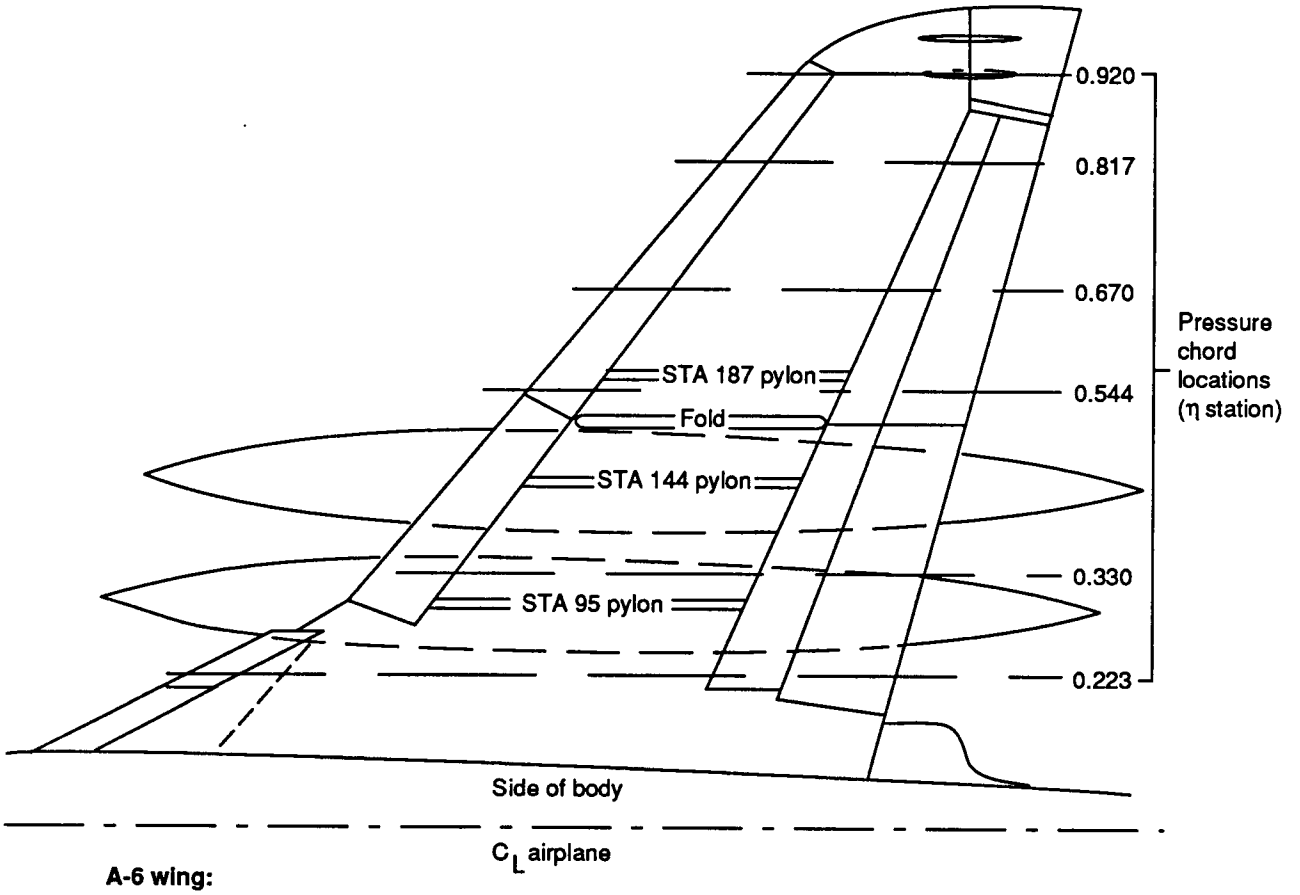

A-6 wing:

- AR = 4.819
- $\Lambda_{LE} = 29.81^{\circ}$
- $\lambda = 0.346$
- $(t/c)_{root} = 0.09$
- $(t/c)_{tip} = 0.059$
- NACA 64A00 x_{mod}

Figure 10. A-6 Wing with External Stores

C9034-01.003-L7160 D18 ai
R1

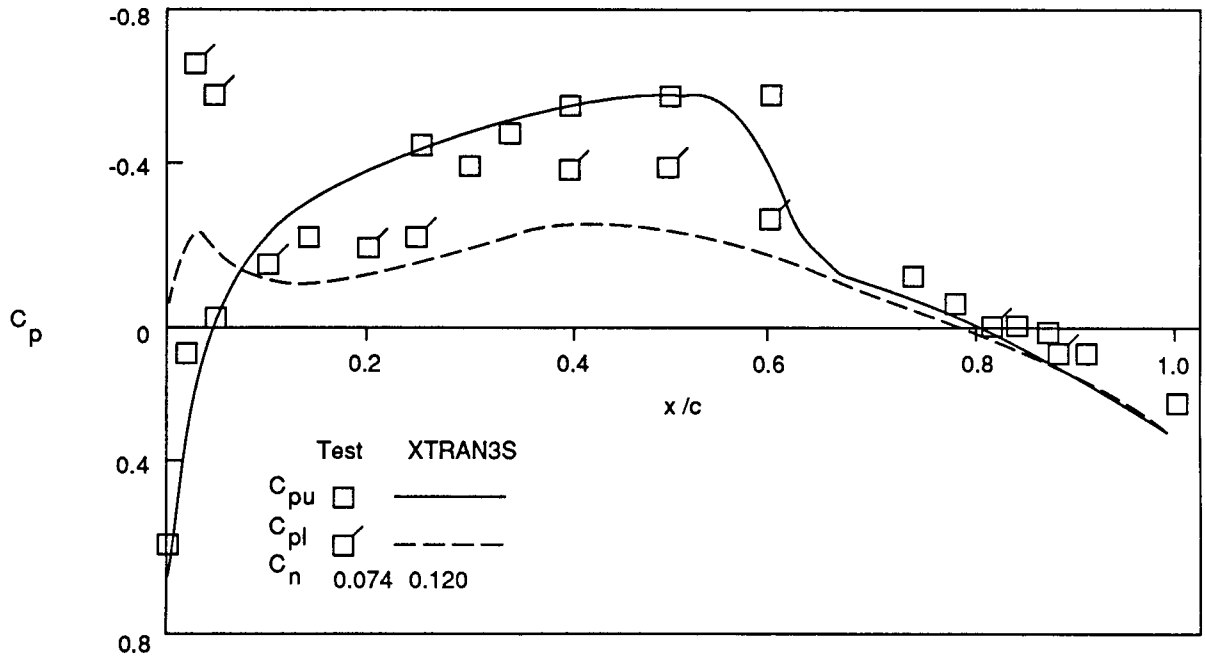

A-6 clean wing:

- M = 0.87
- α = 0.0
- η = 0.33

Figure 11. Comparison of Pressure Distribution on A-6 Wing (Clean)

C9034-01.004-L7160 D18 ai
R1

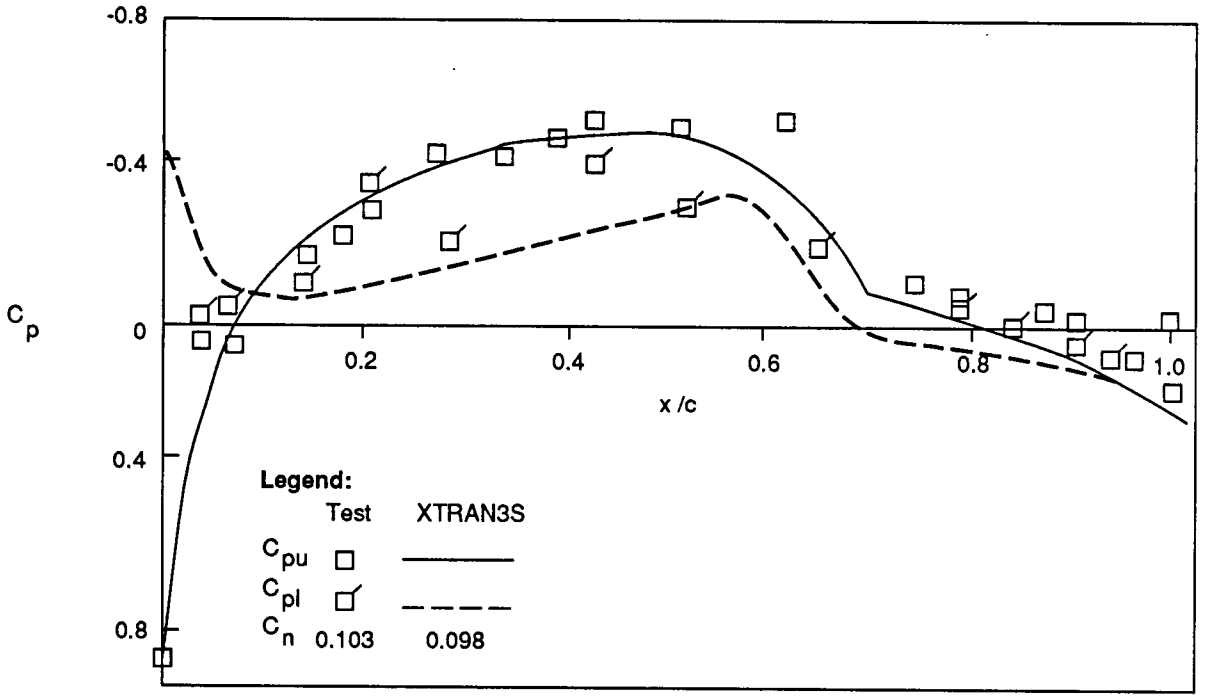

A-6 pylons only:

- M = 0.87
- α = 0.0
- η = 0.33

Figure 12. Comparison of Pressure Distribution on A-6 Wing (Pylons Only)

C9034-01.005-L7160 D18 ai

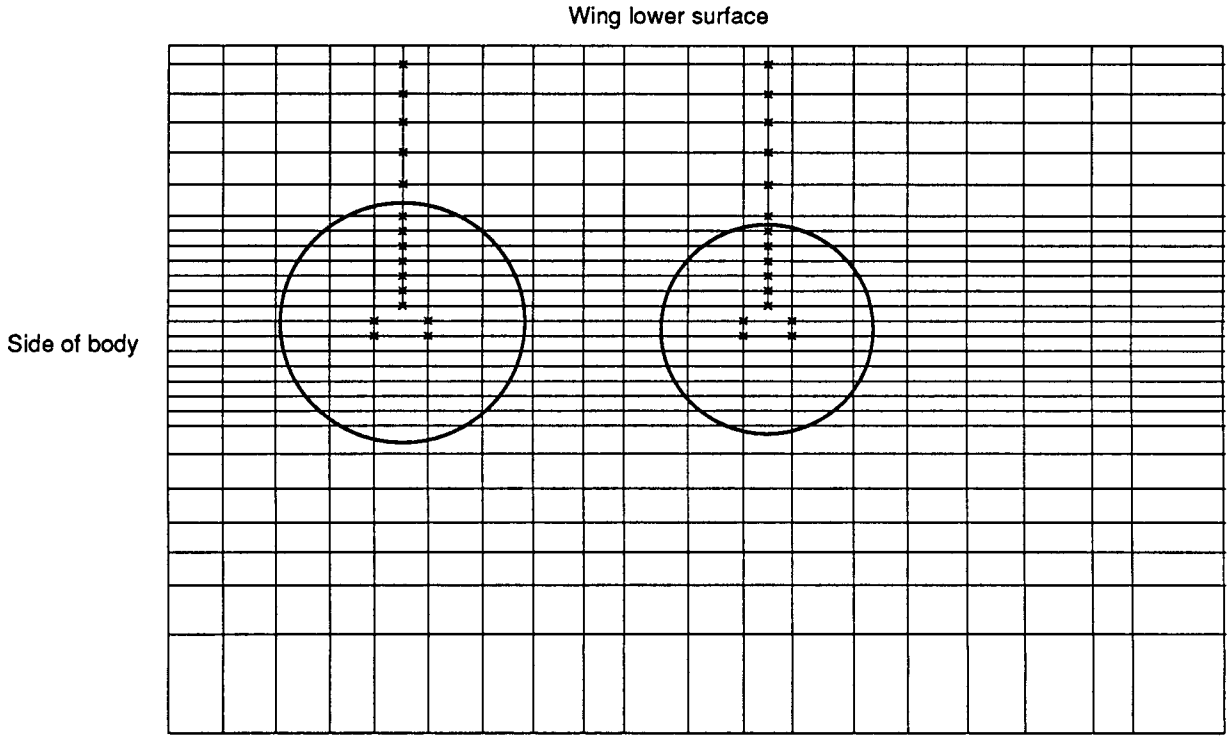

Figure 13. Initial XTRAN3S Store-Pylon Simulation

C9034-01.006-L7160 D18 ai

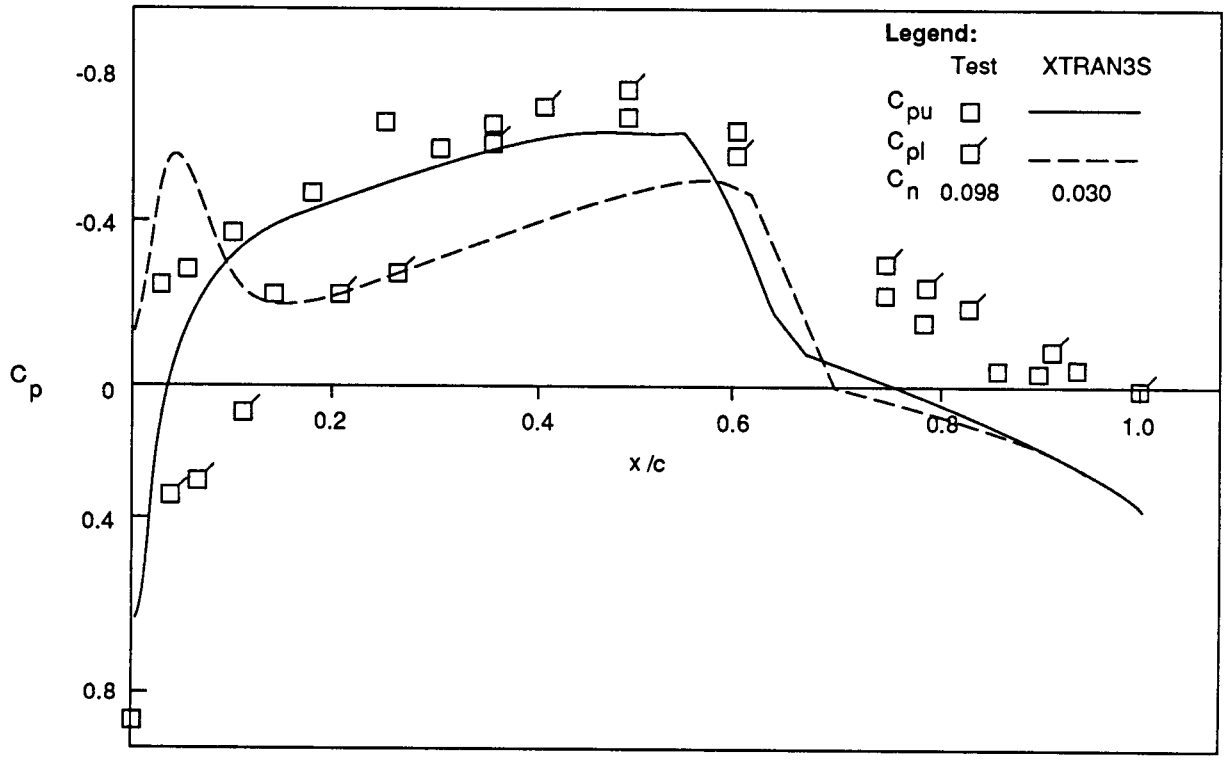

A-6 pylons and stores:

- M = 0.87
- α = 0.0
- η = 0.33

Figure 14. Comparison of Pressure Distribution—A-6 Wing With Stores (Slender Body Approximation)

C9034-01.007-L7160 D18 ai

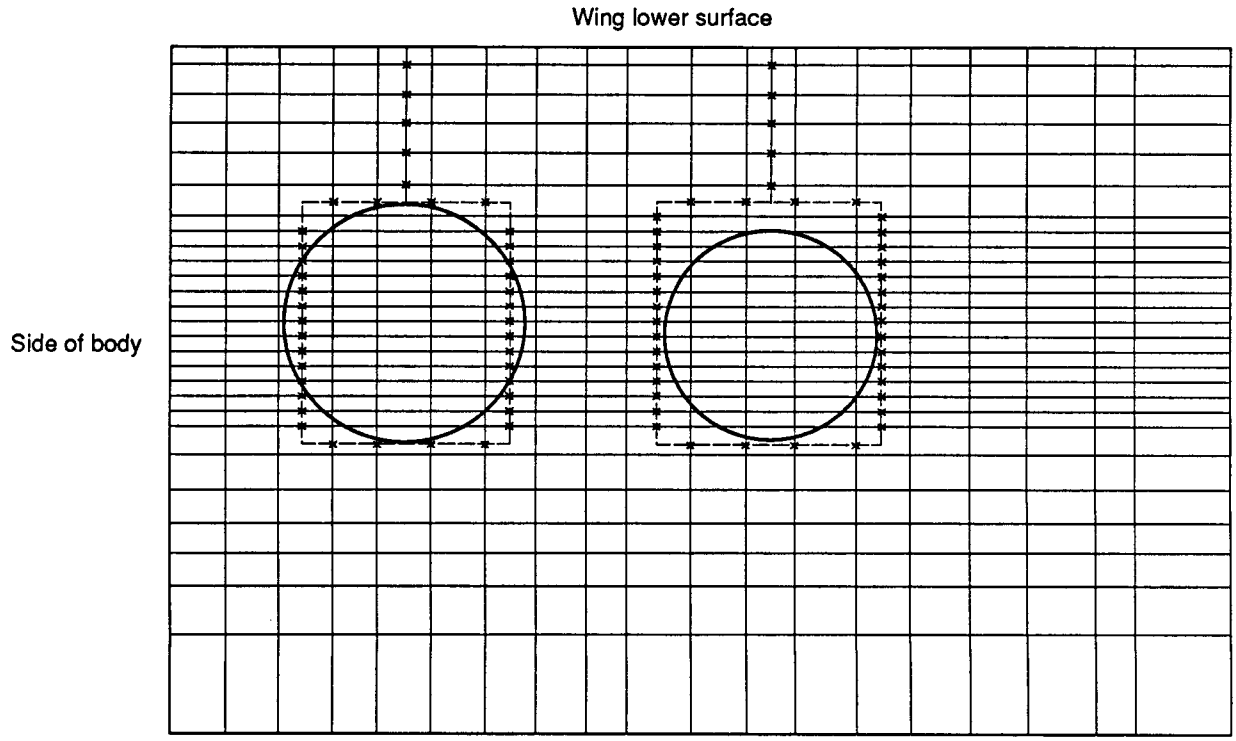

Figure 15. XTRAN3S Store-Pylon Simulation

C9034-01.008-L7160 D18 ai

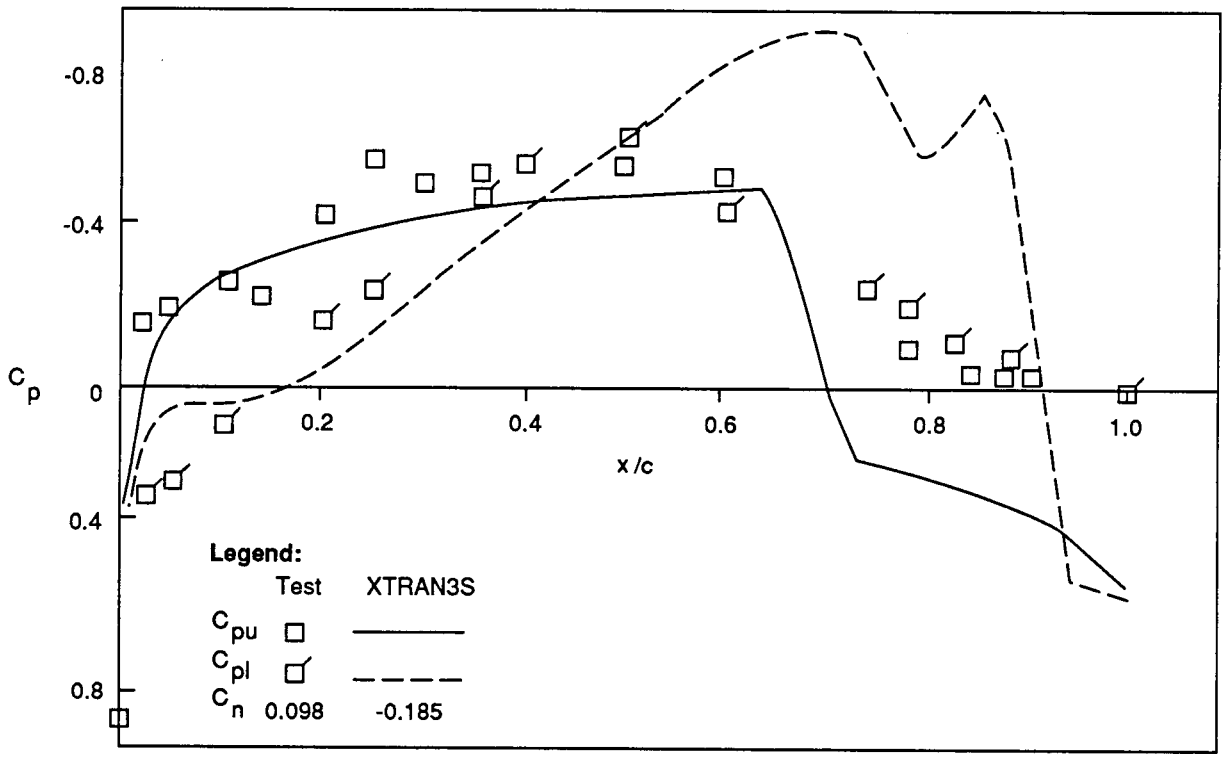

A-6 pylons and stores (interference shell):

- M = 0.87
- α = 0.0
- η = 0.33

Figure 16. Comparison of Pressure Distribution—A-6 Wing With Stores (Interference Shell Approximation)

C9034-01.009-L7160 D18 ai

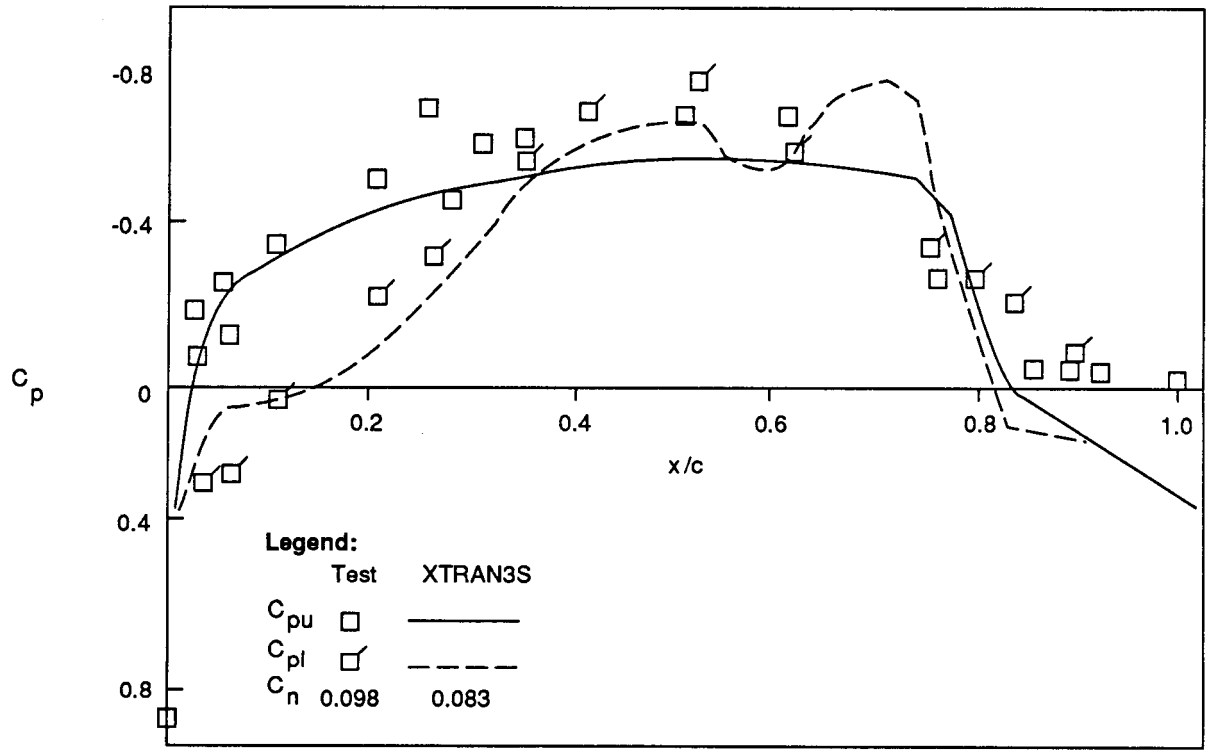

A-6 pylons and stores (interference and aft separation):

- M = 0.87
- α = 0.0
- η = 0.33

Figure 17. Comparison of Pressure Data on A-6 Wing With Stores (Interface Shell and Aft Separation Approximation)

C9034-01.010-L7160 D18 ai

Version case	Wing only	Wing only
1.5	1.00	–
1.5 + W - B	1.05	2.180
1.10	0.43	–
1.10 + W - B	1.69	1.744
1.10 + W - B (vectorized)	0.43	0.450

Note: Normalized Cp sec/iteration

Figure 18. Vectorization of NASA Wing-Body Modification

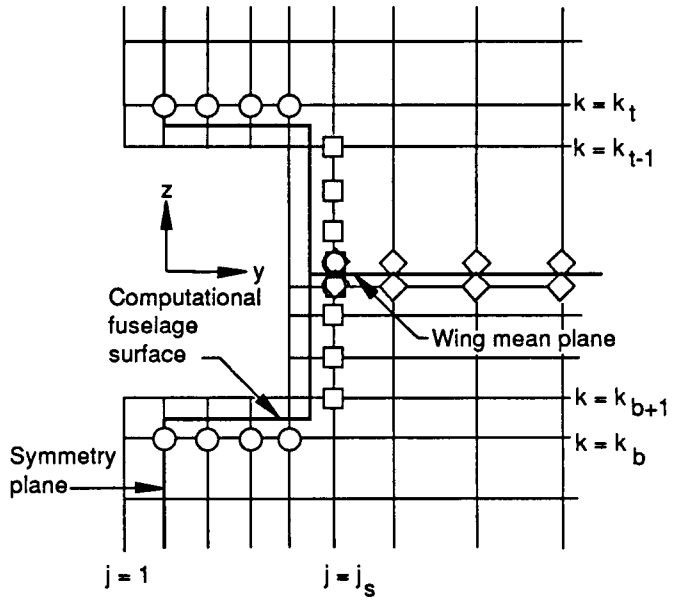

(a) Sectional Grid

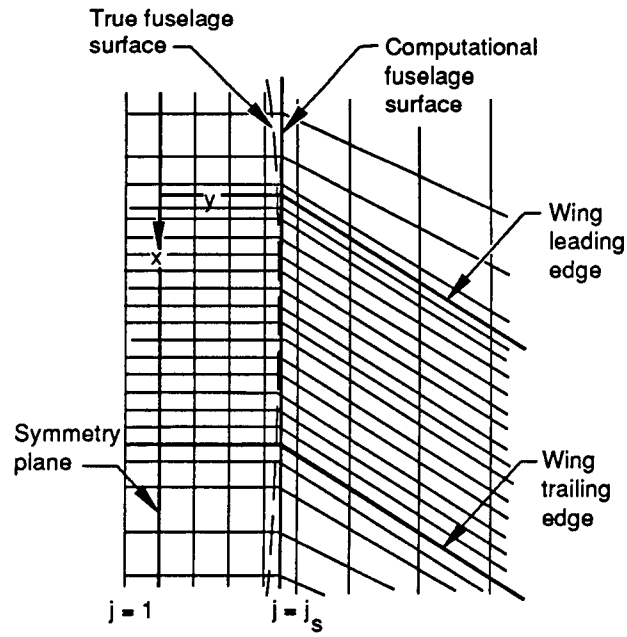

(b) Planform grid

Boundary condition grid points:

○ Fuselage top/bottom

□ Fuselage side

◇ Wing upper/lower

Figure 19. Treatment of Grid to Impose Fuselage Boundary Conditions on Rectangular Interface Shell

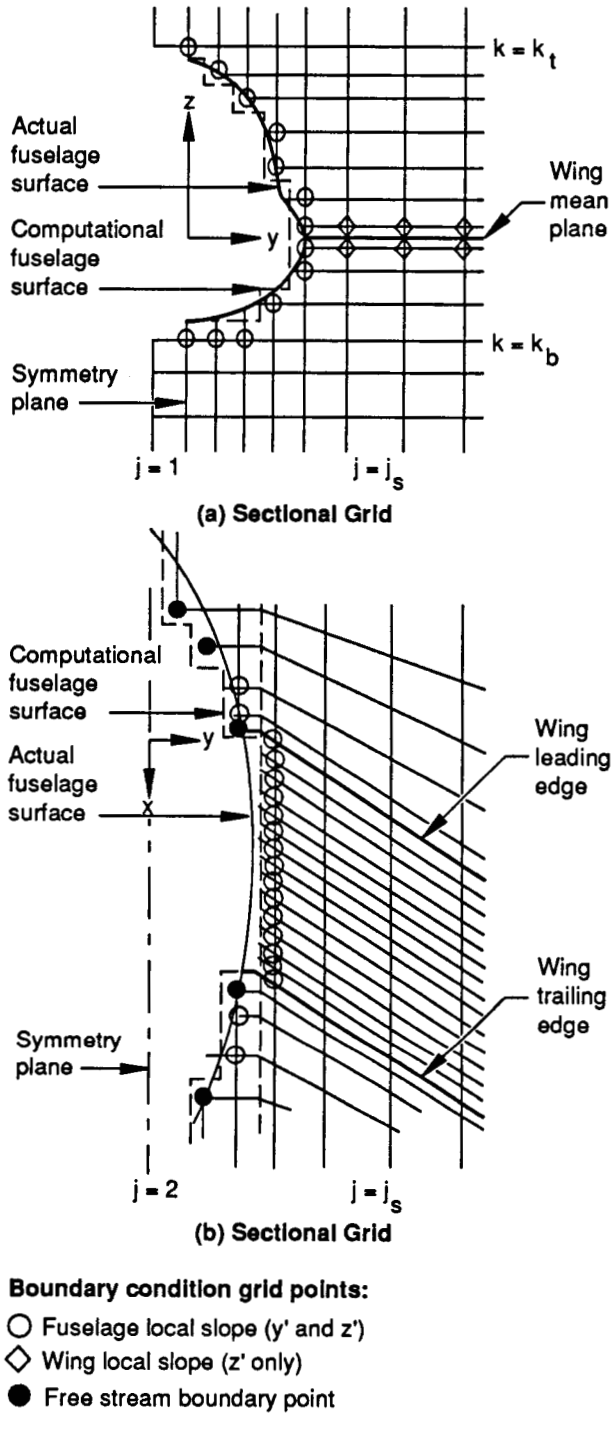

Figure 20. Treatment of Grid to Impose Fuselage Boundary Conditions on Actual Surface Geometry

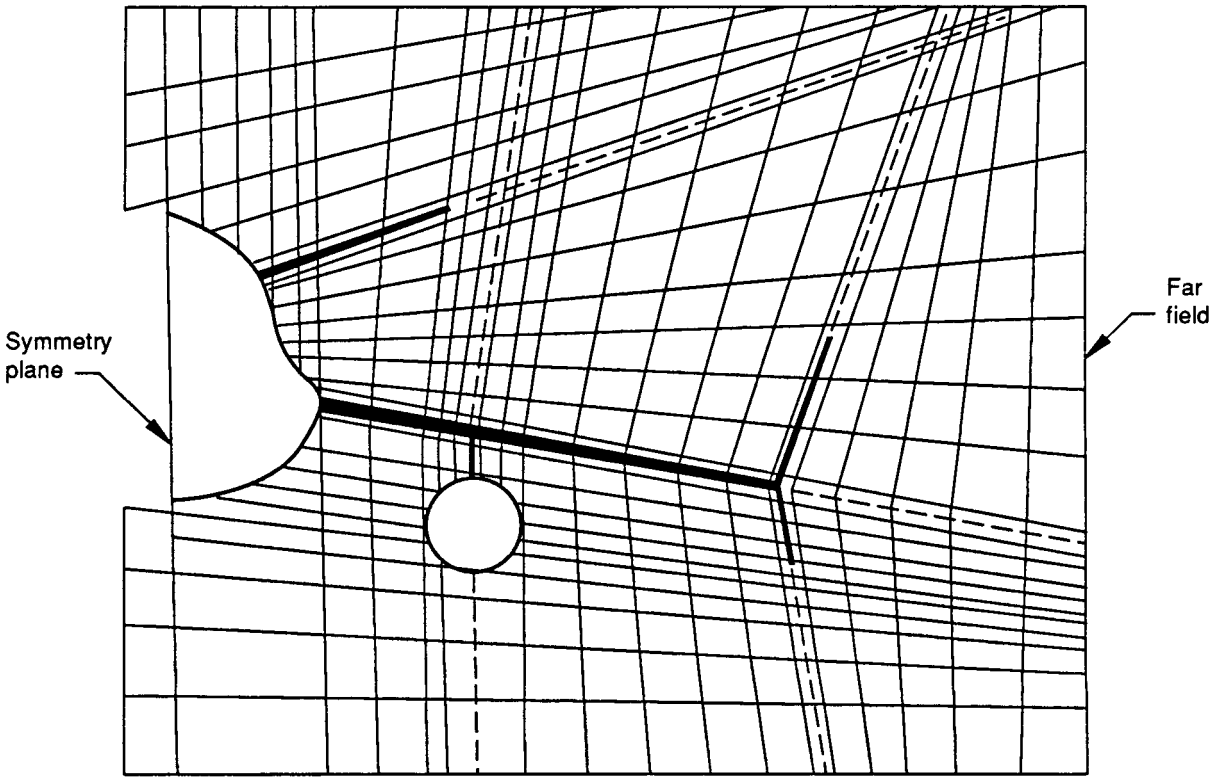

Figure 21. Wing/Fuselage/Canard/Store/Winglet Configuration—Physical Plane

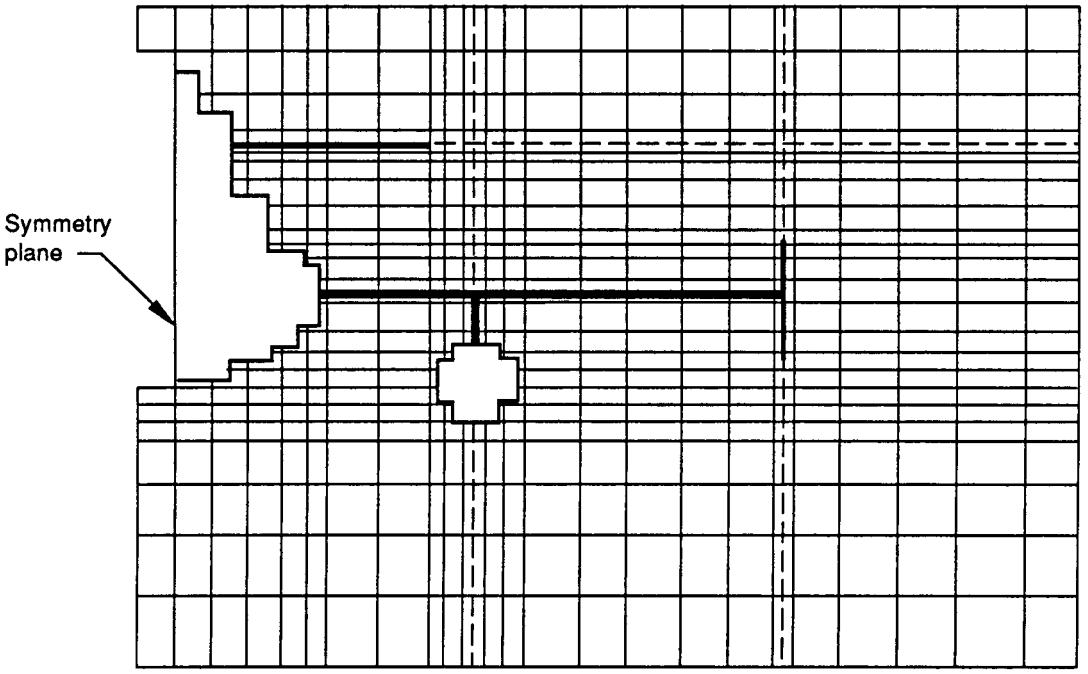

Figure 22. Wing/Fuselage/Canard/Store/Winglet Configuration—Computational Plane

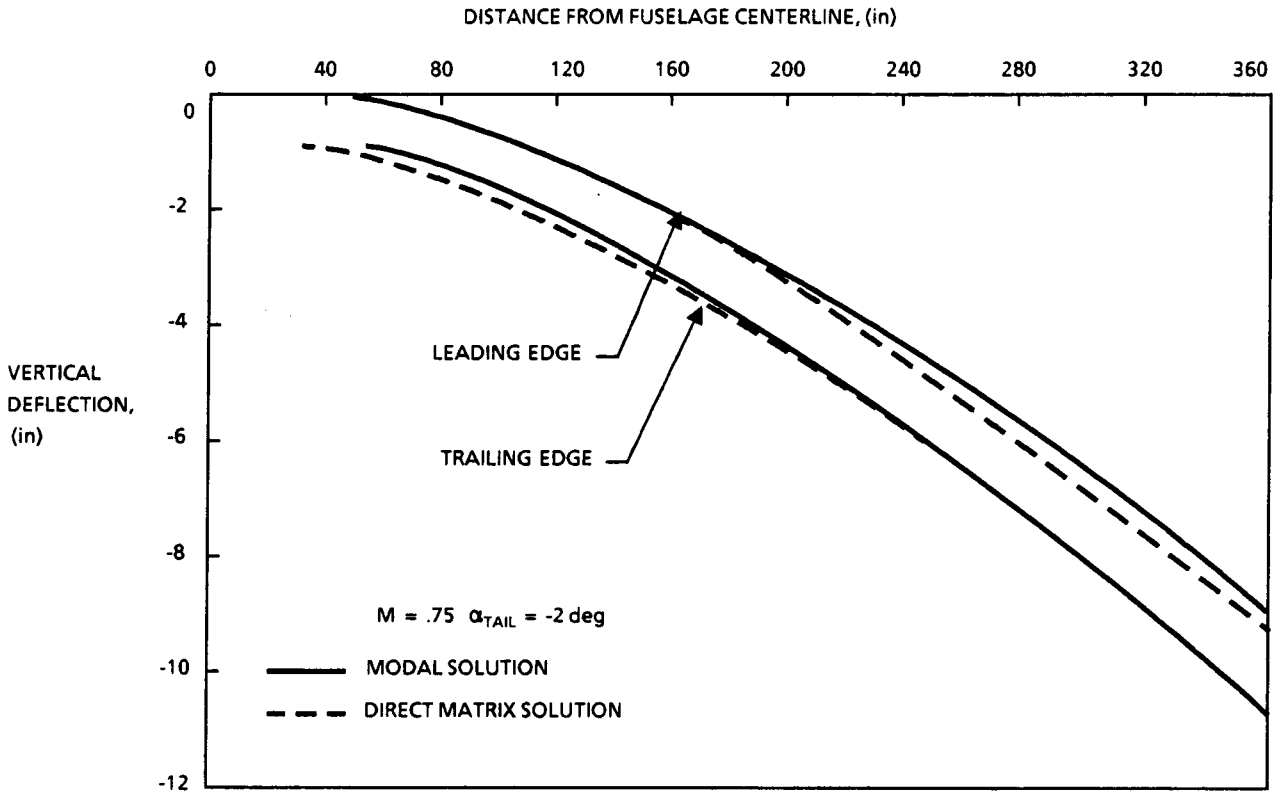

Figure 23. XTRAN3S - Direct Matrix Versus Modal Formulation

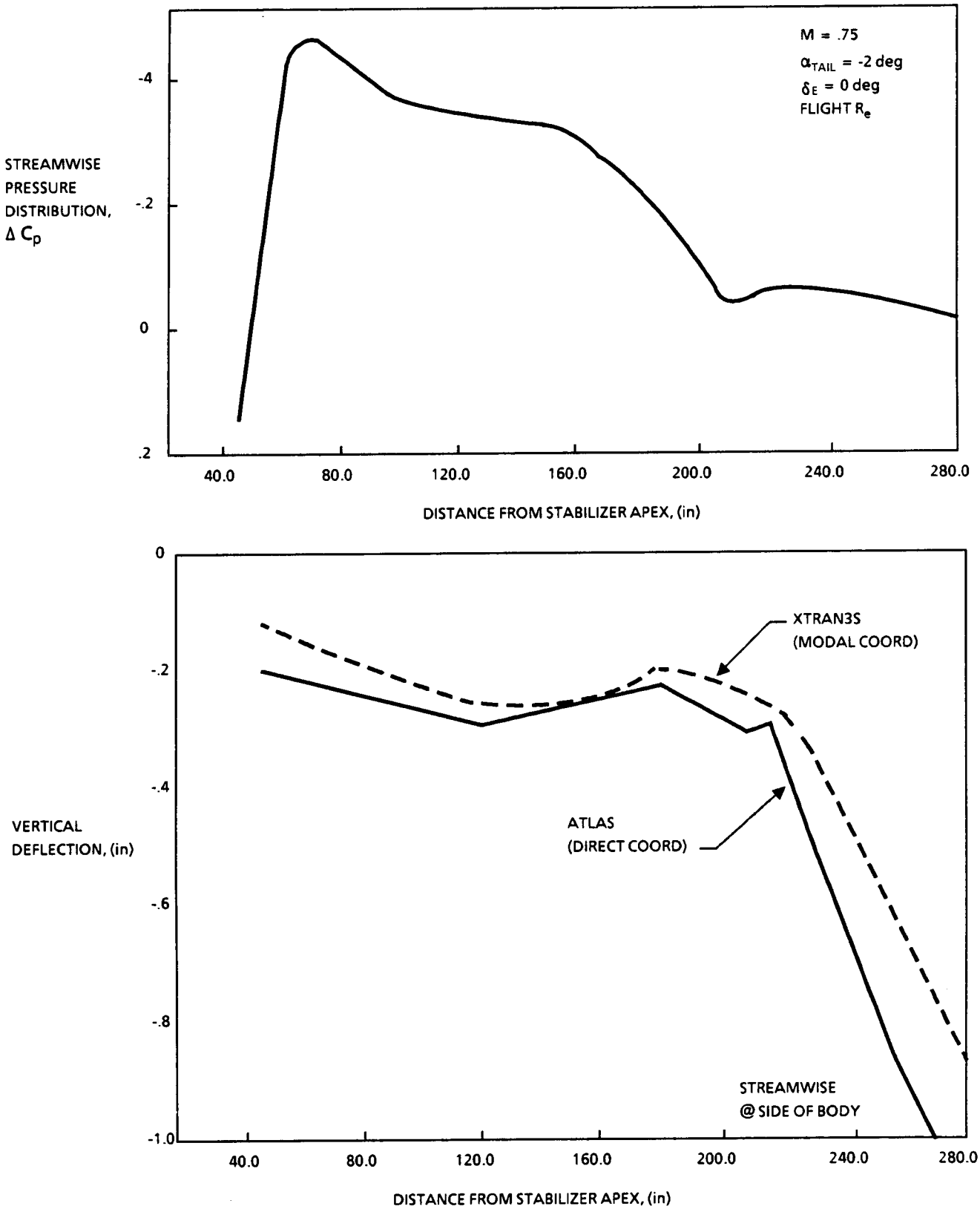

Figure 24. Comparison of XTRAN3S to Atlas Deflections-Identical Pressure Loading